Organic biogeochemical study of deeper southeastern Bengal Basin sediments in West Bengal, India

Behera, Pravat Kumar ; Das, Supriyo Kumar ; Ghosh, Devanita ; Mani, Devleena ; Kalpana, M.S.; Ikehara, Minoru ; Patel, Priyank Pravin

DOI
10.1016/j.orggeochem.2022.104451

Publication date
2022

Document Version
Final published version

Published in
Organic Geochemistry

Citation (APA)
Behera, P. K., Das, S. K., Ghosh, D., Mani, D., Kalpana, M. S., Ikehara, M., & Patel, P. P. (2022). Organic biogeochemical study of deeper southeastern Bengal Basin sediments in West Bengal, India. *Organic Geochemistry*, *170*, Article 104451. https://doi.org/10.1016/j.orggeochem.2022.104451

Organic Geochemistry 170 (2022) 104451

Contents lists available at ScienceDirect

Organic Geochemistry

journal homepage: www.elsevier.com/locate/orggeochem

Organic biogeochemical study of deeper southeastern Bengal Basin sediments in West Bengal, India

Pravat Kumar Behera [a], Supriyo Kumar Das [a,*], Devanita Ghosh [b,c], Devleena Mani [d], M.S. Kalpana [e], Minoru Ikehara [f], Priyank Pravin Patel [g]

[a] Department of Geology, Presidency University, Kolkata, India
[b] Laboratory of Biogeochemistry, Centre for Earth Sciences, Indian Institute of Science, C.V. Raman Avenue, Bangalore 560012, India
[c] Sanitary Engineering Section, Water Management Department, Delft University of Technology, The Netherlands
[d] Centre for Earth, Ocean and Atmospheric Sciences, University of Hyderabad, Telangana 500046, India
[e] National Geophysical Research Institute, Hyderabad, Telangana 500007, India
[f] Center for Advanced Marine Core Research, Kochi University, B200 Monobe, Nankoku 783-8502, Japan
[g] Department of Geography, Presidency University, College Street 86/1, Kolkata 700073, India

ARTICLE INFO

Associate Editor—Alexei Milkov

Keywords:
Bengal Basin
Kerogen type and maturity
Stable isotopes
Methanogenic archaea
Alkanes

ABSTRACT

The Bengal Basin is a fluvio-deltaic basin spanning Bangladesh and part of east and northeast India. The evolution of the peripheral foreland basin has been studied, but published literature on depositional conditions, source and maturity of organic matter in the deeper sediments of the Indian section of the basin is rare, despite the fact that natural gas is often encountered during hydrocarbon exploration. Our research assesses the depositional environment and source of the organic matter (OM) in the Pleistocene-Miocene sediments from five wells drilled by Oil and Natural Gas Corporation Limited in the southeastern Bengal Basin, West Bengal, India and aims to understand its maturity and potential to yield natural gas. The total organic carbon/nitrogen ratio and stable isotope ($\delta^{13}C$ and $\delta^{15}N$) signature indicate primarily aquatic and C_3 terrestrial plant sources of the OM and deposition under tidal flat and marshy environments. The *n*-alkane and isoprenoid alkane distribution are consistent with an autochthonous source of OM and terrestrial oxic-suboxic shallow-water depositional setting. The Rock-Eval parameters, such as maximal pyrolysis temperature, hydrogen and oxygen indices, indicate the immature nature of Type III and Type IV kerogen. The presence of methanogenic archaea, as indicated by phylogenetic analysis, in two Miocene sediment samples from one well indicates an active microbial activity in Type III immature OM, derived from C_3 marsh vegetation and deposited under oxic shallow-water conditions. Our research describes the presence of methanogenic archaea for the first time in Miocene Bengal Basin sediments and is one of the few reports of their presence in deep (> 4000 m) horizons.

1. Introduction

The Bengal Basin, formed via the Indian continent-Eurasian continent collision in the Eocene, is a complex foreland basin (Mukherjee et al., 2009). It is situated at the conjunction of the Indian craton to the west, the Himalayan belt and Shilong massif to the north and the Indo-Burman ranges to the east (Uddin and Lundberg, 1998). The basin shows noticeable variability in Neogene sediment thickness, indicating a complicated tectonic and depositional history (Hossain et al., 2019). According to Desikachar (1974), the Bengal Basin is a pericratonic basin of the Indian plate. Tectonically, the basin is divided into two broad parts by the Hinge zone: (1) the Stable shelf (Indian platform) to the northwest and west and (2) the deeper part of the basin (Bengal foredeep) in the south and east (Sengupta, 1966; Uddin and Lundberg, 1998). Today, the major portion of the basin lies in Bangladesh and covers parts of three Indian states, namely West Bengal, Tripura and Assam (Hossain et al., 2019).

Sedimentation in the basin started from the late Eocene (Uddin and Lundberg, 1998; Najman et al., 2008). A major phase of clastic sedimentation from the northeast, started in the early Miocene, led to the formation of the major Mio-Pliocene delta complex (Uddin, 1990). The Miocene-Pliocene-Pleistocene depositional environments are dominated by brackish-estuarine-deltaic conditions and marginal marine conditions inferred from micropaleontological study in the Jessore depression

* Corresponding author.
E-mail address: sdas.geol@presiuniv.ac.in (S.K. Das).

https://doi.org/10.1016/j.orggeochem.2022.104451
Received 28 February 2022; Received in revised form 15 May 2022; Accepted 2 June 2022
Available online 9 June 2022

and Surma Basin in Bangladesh (Banerji, 1984). The Ganges and Brahmaputra rivers transport the clastic sediments derived from the Himalayas and deposit them in the Ganges-Brahmaputra deltaic system (Hossain et al., 2009). Stratigraphy, sedimentation and tectonic history of the basin have been studied in detail in the northeastern part of the basin that reveals that Miocene sedimentation has changed from flysch to molasse (Alam, 1989; Johnson and Alam, 1991). Also, a tide-dominated shallow marine sedimentation during the Miocene in the

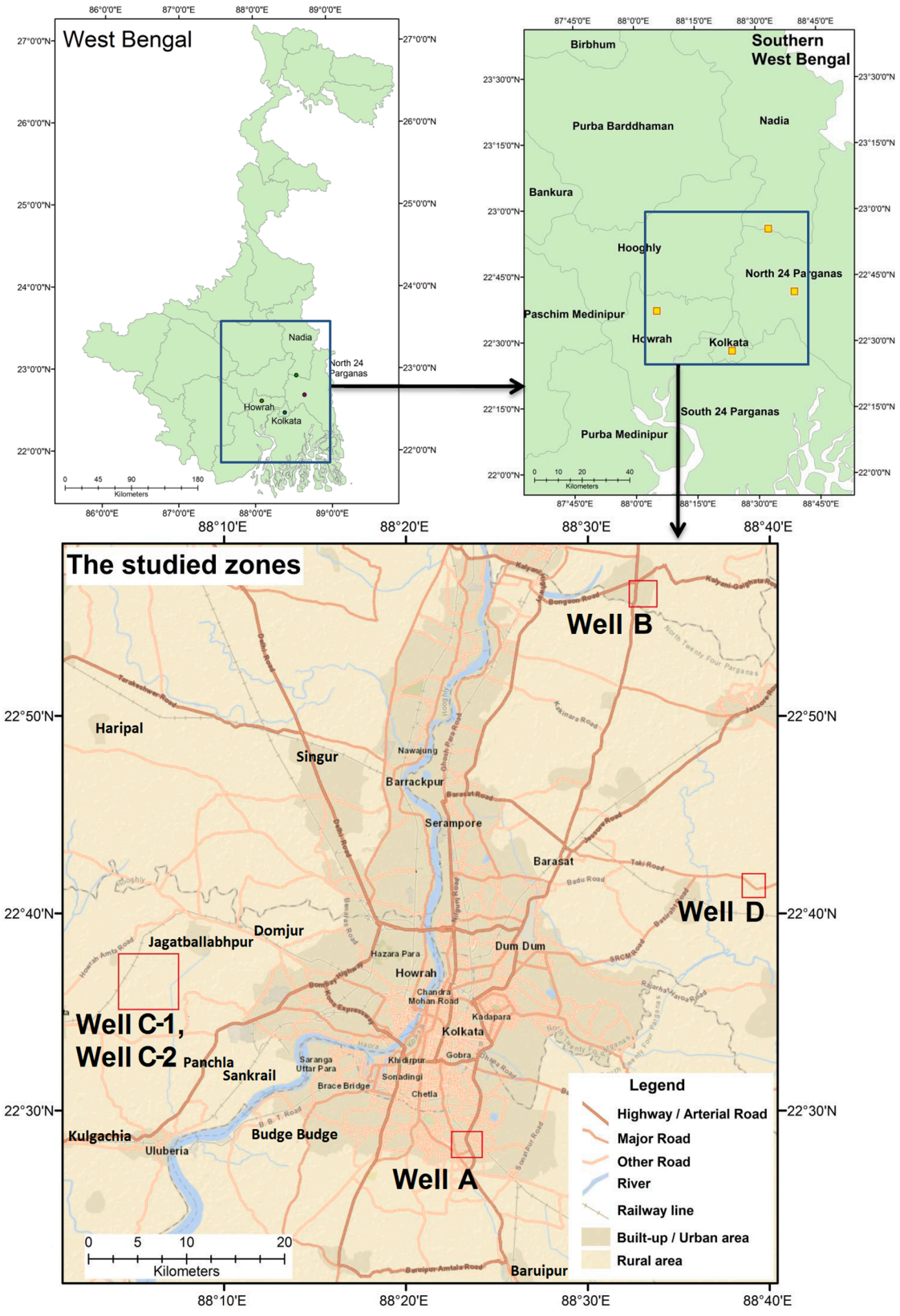

Fig. 1. Position of the ONGC wells in West Bengal, India.

southeastern Bengal Basin has been postulated (Alam, 1995). Hossain et al. (2009) have inferred anoxic to sub-oxic depositional conditions of the Miocene-Pleistocene sediments with decreasing terrestrial higher plant organic matter (OM) input in the Sylhet Basin (a sub-basin of the Bengal Basin in Bangladesh) using elemental carbon (C), nitrogen (N), sulfur (S), Rock-Eval pyrolysis and gas chromatography–mass spectroscopy (GC–MS).

The thick (±22 km) sedimentary succession of the early Cretaceous to Holocene lead to significant attention to hydrocarbon exploration in the Bengal Basin (Curray, 1991; Curray and Munasinghe, 1991). Hydrocarbon exploration has been extensively carried out by the Bangladesh Oil, Gas and Mineral Corporation (BOGMC, 1997) in the last few decades, and an economic quantity of natural gas has been reported in the Bangladesh section of the Bengal Basin (Bengal Foredeep), where terrestrial OM at an early maturation stage is considered as the source of the gas (Imam and Hussain, 2002; Islam, 2009).

The Indian section of the Bengal Basin is also considered as geologically prospective for hydrocarbon generation, and over 50 wells have been drilled during the last three decades under the Indo-Stanvac Petroleum Project and by the Oil and Natural Gas Corporation (ONGC) Limited (Banerji et al., 1990). The majority of the gas indications in the drilled wells under the Indo-Stanvac Petroleum Project have been associated with Miocene sediments (Ramaswamy, 1962). The ONGC has reported natural gas from several deeper (> 2000 m) wells in West Bengal (Directorate General of Hydrocarbons, 2019) although, unlike Bangladesh, published reports on the paleodepositional conditions and source and maturity of sedimentary OM in the Indian section of the Bengal Basin are rare (e.g., Babu, 1976; Roybarman, 1984; Bastia, 2006).

The objectives of the present study were to evaluate the sources and depositional environment of the OM in the selected deep Bengal Basin sediments and to understand its potential for natural gas (thermogenic/biogenic) generation by studying the stable isotopes of organic carbon ($\delta^{13}C$) and nitrogen ($\delta^{15}N$), aliphatic hydrocarbons (alkanes) and kerogen maturity. We attempted mapping the phylogenetic diversity of methanogenic species to understand biogenic methane production in the deeper Bengal Basin sediments.

2. The Bengal Basin

The Bengal Basin (Fig. 1) is one of the largest fluvio-deltaic basins (~200,000 km^2; Alam et al., 2003) in the world. The peripheral foreland basin is situated at the confluence of the Brahmaputra and Ganga rivers. The Bengal Fan, the largest deep-sea fan complex on Earth (Rea, 1992), is further developed into the Bay of Bengal (Morgan and McIntire, 1959; Babu, 1976; Allison, 1998). The basin lies in the Himalayan foreland at the junction of the Burmese, Eurasian and Indian plates (Mukherjee et al., 2009).

Drilling in the Bengal Basin has revealed sedimentary sequences ranging in age from Cretaceous to recent (Basu, 1962) (Table 1). Sengupta (1966) summarises that the depositional environment of the Bengal Basin has changed sharply to a foredeep from a stable shelf condition. A deep seismic hinge zone (Eocene hinge zone) separates the two depositional environments (Mukherjee et al., 2009). Gondwana basement underlies the Bengal Basin sediments, and the thickness of the sediments varies between the foredeep (> 16 km) and stable shelf (8 km). The basin was formed during the late Jurassic period and major tectonic movements, such as the Dauki fault and Naga thrust, occurred during the Late Cretaceous, Eocene and Miocene with the regression of the sea during the late Miocene and early Pliocene (Sengupta, 1966).

The Pleistocene and Pliocene sequences in the Bengal Basin primarily belong to the Ranaghat Formation and mostly contain claystone, siltstone and pebbly sandstone, whereas the Miocene Debagram and the Pandua Formations are characterised of claystone, siltstone, sandstone and shale (Banerji, 1984; Alam et al., 2003) (Table 1). The Ranaghat Formation is characteristic of marginal marine with occasional interdeltaic settings, while the Debagram Formation exhibits a mixed estuarine to marginal deltaic facies character (Banerji, 1984). On the contrary, the presence of planktonic and benthic foraminifera in the Pandua Formation indicates a short span of marine transgression during the Miocene (Banerji, 1984).

3. Methods

3.1. Samples

Ninety-three cutting samples belonging to the Ranaghat (Pleistocene to Pliocene), Debagram and Pandua formations (Miocene) from five wells, namely Well A, Well B, Well C-1, Well C-2 and Well D (Table 2; Fig. 2), in the Bengal Basin were provided by the Keshava Deva Malaviya Institute of Petroleum Exploration (KDMIPE) in Dehradun. Sample selection was based on the previous observation of the presence of natural gas (unpublished ONGC report). Dry samples were stored under dry and dark conditions at KDMIPE. The samples were recovered by ONGC Limited. However, the precise location of the wells cannot be disclosed due to proprietary reasons. Agate mortar and pestle were used to homogenise the samples. Total organic carbon (TOC), $\delta^{13}C$ and $\delta^{15}N$, *n*-alkane and kerogen maturity analyses were performed on the samples.

3.2. Rock-Eval pyrolysis

Free hydrocarbons (S_1) and thermogenic hydrocarbons (S_2), released prior to and during the thermal cracking of kerogen, respectively, were measured using a Rock-Eval 6 pyrolyzer, Turbo version (Vinci Technologies). Sample analysis using the Rock-Eval 6 analyser further yielded TOC content and temperature (Tmax) at which the maximum S_2 was liberated as well as the amount of CO_2 produced (S_3) during kerogen pyrolysis in the absence of O_2. Oxygen index (OI) and Hydrogen index

Table 1
Stratigraphic succession of the Southwestern part of the Bengal Basin (Alam et al., 2003; Chandra et al., 1993; Roy and Chatterjee, 2015).

Chronostratigraphy	Group	Formation	Lithology	Depositional Environment
Holocene		Alluvium	Sand, clay, gravel	
Pleistocene-Late Pliocene	Barind	Barind	Clay, minor sand	Fluvial-alluvial and prograding delta-shelf
Early Pliocene-Middle Miocene	Bhagirathi	Debogram/Ranaghat	Sandstone, siltstone and shale	
		Pandua/Malta	Sandstone/mudstone	
Oligocene	Jayantia	Memari/Burdwan	Sandstone/mudstone	Delta front to shelf and slope
Late Eocene		Kopili	Shale, mudstone, sandstone	
Middle Eocene		Sylhet Limestone	Limestone with sandstone	Carbonate platform
Paleocene		Jalangi	Sandstone, mudstone	Deltaic to outer shelf
Early to Late Cretaceous	Rajmahal	Ghatal	Sandstone, limestone, shale	
		Bolpur	Mudstone, sandstone, trapwash	Coastal to fluvial-alluvial
		Dhananjaypur	Grey shale	
		Rajmahal Trap	Basalt, andesite, intertrappeans	Subaerial lava flows

Basement: Precambrian Shield rocks along with the cover Gondwana formations.

Table 2
Sampling depth intervals of the studied ONGC wells.

Sl. No	Well A (m)	Well B (m)	Well C-1 (m)	Well C-2 (m)	Well D (m)
1	655–660	1145–1150	860–865	1805–1810	3105–3110
2	760–765	1345–1350	960–965	1900–1905	3195–3200
3	805–810	1545–1550	1055–1060	2000–2005	3230–3235
4	860–865	1745–1750	1145–1150	2100–2105	3365–3370
5	900–905	1945–1950	1245–1250	2200–2205	3460–3465
6	960–965	2145–2150	1360–1365	2300–2305	3603–3608
7	1005–1010	2340–2345	1460–1465	2400–2405	3720–3723
8	1060–1065	2540–2545	1560–1565	2500–2505	3801–3804
9	1105–1110	2740–2745	1660–1665	2605–2610	3900–3903
10	1160–1165	2940–2945	1760–1765	2700–2705	4050–4053
11	1205–1210	3140–3145	1865–1870	2800–2805	4138–4141
12	1260–1265	3340–3345	1960–1965	2900–2905	4231–4234
13	1305–1310	3545–3550	2060–2065		4323–4326
14	1360–1365	3735–3740	2160–2165		4416–4419
15	1405–1410	3945–3950	2260–2265		4500–4503
16	1460–1465	4150–4155	2360–2365		4659–4662
17	1505–1510		2460–2465		4752–4755
18	1560–1565		2560–2565		4851–4854
19	1600–1605		2660–2665		4923–4926
20	1660–1665		2765–2770		4998–5001
21	1705–1710		2860–2865		
22	1725–1730		2960–2965		
23			3095–3100		

(HI) were estimated following Lafargue et al. (1998) and Behar et al. (2001). Calibration of the analyser was performed in the standard mode using IFP Standard, 160,000 (Tmax = 416 °C, S_2 = 12.43). The Rock-Eval pyrolysis was performed at the National Geophysical Research Institute (NGRI) in Hyderabad.

3.3. Stable isotope analysis

The TOC and total N were measured using an Automated Nitrogen Carbon Analyser - Solids and Liquids (ANCA-SL) elemental analyser (EA). The elemental analyser, coupled to a Europa 20–20 isotope ratio mass spectrometer (IRMS), was used for $\delta^{13}C$ and $\delta^{15}N$ analyses. Prior to the TOC and $\delta^{13}C$ analyses, the samples were acidified with 2 M hydrochloric acid and left overnight to allow inorganic carbon to be liberated as CO_2. The samples were neutralised by repetitively washing with distilled water and subsequently oven-dried at 60 °C in readiness for $\delta^{13}C$ analysis. Results were expressed in the conventional δ notation (‰) using standards calibrated against the international Vienna PeeDee Belemnite (V-PDB) for $\delta^{13}C$ and atmospheric N_2 for $\delta^{15}N$. The results of the $\delta^{13}C$ and $\delta^{15}N$ analyses were calculated as follows:

$$\delta\ (‰) = [(R_{sample}/R_{standard}) - 1] \times 1000$$

For $\delta^{13}C$ analysis, the R_{sample} and $R_{standard}$ are the $^{13}C/^{12}C$ ratio of the sample and standard, respectively. For $\delta^{15}N$, the R_{sample} and $R_{standard}$ represented the $^{15}N/^{14}N$ ratio of the sample and atmospheric N_2, respectively. Internal standards and blanks were analysed in between every eight samples. Duplicate analysis was performed in 20% of the samples.

For carbon isotope analysis, IA-R001 (wheat flour, $\delta^{13}C$ = of −26.4‰) was used as the reference material. Check samples, namely IA-R005 (beet sugar, $\delta^{13}C$ = –26‰) and IA-R006 (cane sugar, $\delta^{13}C$ = –11.6‰), were used for quality control. The reference material and check samples were calibrated against the IAEA-CH-6 (sucrose, $\delta^{13}C$ = –10.4‰), which was distributed by the International Atomic Energy Agency (IAEA) in Vienna.

IA- R001 (wheat flour; $\delta^{15}N$ = 2.5‰) was used as reference material for $\delta^{15}N$ analysis. Check samples, IA- R001, IA-R045 (ammonium sulphate; $\delta^{15}N$ = –4.7‰), IA-R046 (ammonium sulphate; $\delta^{15}N_{AIR}$ = 22‰) and IA-R069 (Tuna protein; $\delta^{15}N$ = 11.6‰), were used for quality control. The reference material and check samples were calibrated against an inter-laboratory comparison standard, IAEA-N-1 (ammonium sulphate; $\delta^{15}N$ = 0.4‰), distributed by the IAEA, Vienna. The precision of the analyses (10 replicated standards) was 0.3% for C, 0.03% for N, 0.06‰ for $\delta^{13}C$ and 0.18‰ for $\delta^{15}N$. Duplicate analyses show a reproducibility value of 0.1‰. Stable isotope analyses of the samples were performed at Iso-Analytical Limited in the UK.

3.4. Aliphatic hydrocarbons extraction and analysis

A total of 22 samples (4 from Well B, 1 from Well C-1, 3 from Well C-2 and 14 from Well D) were selected for the hydrocarbons extraction. Samples with TOC ≥ 0.5% were selected for the extraction because hydrocarbons (gas/condensates) generation is reported from the Bengal Foredeep region of the Bengal Basin in Bangladesh only in sediments with TOC ≥ 0.5% (Shamsuddin and Khan, 1991). A mixture (3:1, v/v) of dichloromethane and methanol was used to extract hydrocarbons from the homogenised sediments by ultrasonication (Wu et al., 2014). The extract was concentrated using a rotaevaporator under a near-vacuum. The concentrated extract was evaporated to dryness under nitrogen. The aliphatic hydrocarbon fraction, containing normal alkanes (*n*-alkanes), was eluted with hexane using column chromatography (Zhang et al., 2004). The aliphatic hydrocarbon fractions were stored in GC vials until analysis.

Analysis of alkanes was performed using an Agilent 6890 N gas chromatograph (GC) equipped with a 25 m HP-ULTRA 2 fused silica capillary column (0.200 mm i.d.) and coupled to an Agilent 5973 Network Mass Selective Detector. The oven temperature was programmed from 50 °C to 120 °C at 30 °C/min and from 120 °C to 310 °C at 6 °C/min followed by an isothermal period of 25 min. The carrier gas was helium. Compound identification was achieved by comparing the GC retention times, fragmentation patterns, and *m/z* peaks (*m/z* = 57, 71) of ions and published mass spectra (Peters et al., 2005). An Agilent 7890B GC system equipped with an Agilent CP-Sil 5 CB column (60 m × 250 μm × 0.10 μm) and flame ionisation detector was used for quantification.

3.5. Environmental DNA extraction

Total environmental DNA in the four sediment samples collected from Well D (4138–4141 m, 4659–4662 m, 4923–4926 m and 4998–5001 m) were extracted using the standard protocol as described by Tringe and Rubin (2005) and Liles et al. (2009). The humic acid and extractable organic matter were removed using GenElut columns (Merck), and the microbial cells were lysed by the alkaline lysis method. The cell debris was removed, and DNA was precipitated using Na acetate in 100% ethanol overnight at −20 °C. The purity and concentration of the DNA were examined on 1% agarose gel horizontal electrophoresis and quantification of the DNA was performed using a Qubit® dsDNA HS Assay Kit. Samples with TOC content > 1% only had sufficient DNA for downstream molecular analysis.

3.5.1. Polymerase chain reaction (PCR) amplification of partial mcrA and aprA gene

Amplification of partial *mcrA* gene and *aprA* fragments was performed in extracted DNA samples using the McrA and AprA primers. Each PCR reaction included 0.5 μL (~20 ng) DNA template, 10X Dream *Taq* buffer (5.0 μL; Thermo), dNTPs (5.0 μL; 0.2 mM final concentration), 5.0 $MgCl_2$ (μL; 2.0 mM final concentration), 0.5 μL of *mcrA* primers (M13F, 5′-TGTAAAACGACGGCCAGTGGTGGTGTMGGATTCACACARTAYGCWACAGC-3′ and M13R, 5′-CAGGAAACAGCTATGACCTTCATTGCRTAGTTWGGRTAGTT-3′) (Luton et al., 2002) or *aprA* primers (AprA-1-FW, 5'-TGGCAGATCATGATYMAYGG- 3′ and AprA-5-RV, 5′- GCGCCAACYGGRCCRTA-3') with a final concentration of 5 μM (Meyer and Kuever, 2007). Dream *Taq* polymerase (0.5 μL; 5 U/μL; Fermentas) was used as the key polymerase enzyme, and nuclease-free water was used to keep the final reaction volume to 50 μL. The reaction conditions were set according to methods suggested

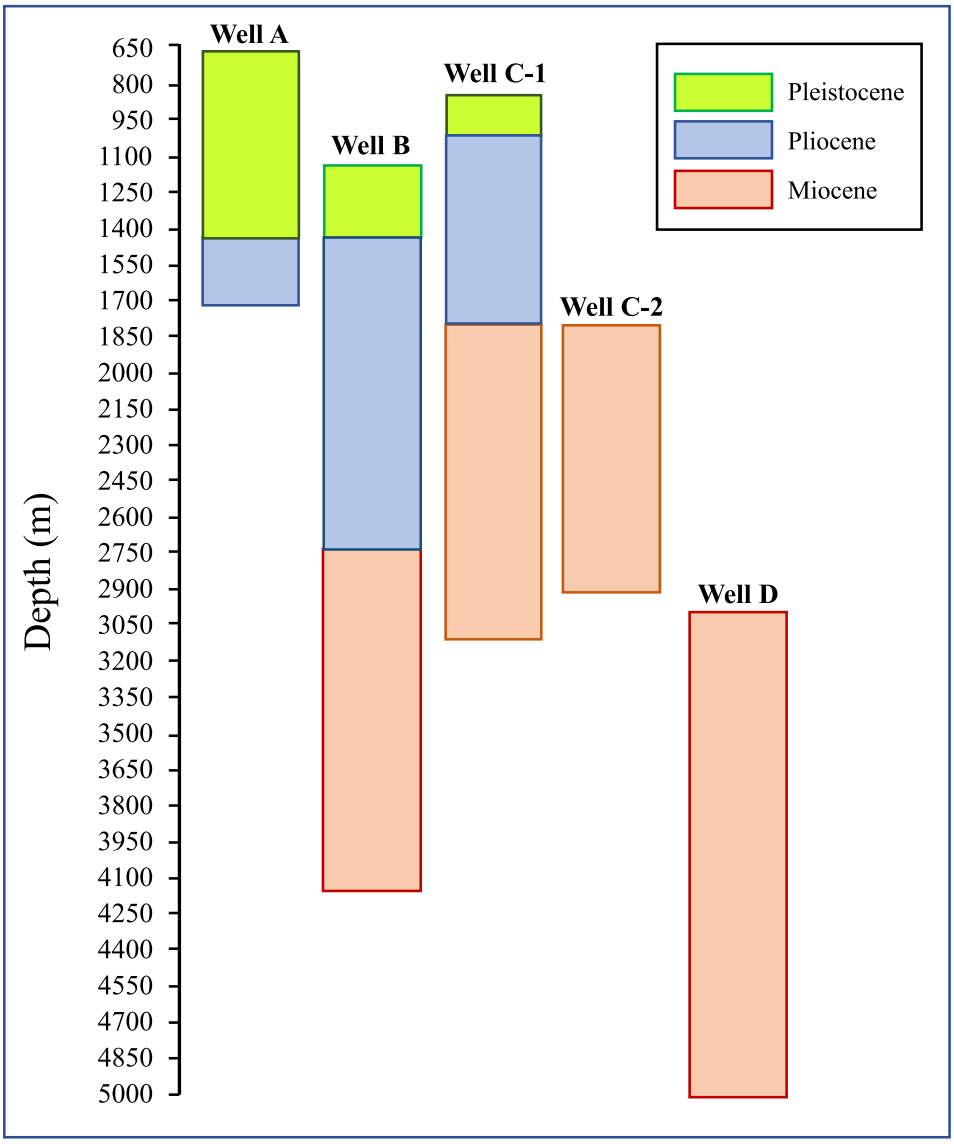

Fig. 2. Sampled sections of Pleistocene, Pliocene and Miocene intervals in the drilled wells (not in scale).

by Luton et al. (2002) and Meyer and Kuever (2007) for the respective primer-based reactions.

All the PCR reaction products were pooled from the triplicate sets and purified by using PCR product Gel Purification Kit following the instruction of the manufacturer (Qiagen).

3.5.2. Clone library preparation and sequencing

Cloning of the amplified and purified PCR products in *Escherichia coli* strain DH5α was performed using pGEM®-T Easy cloning vector (Promega). From positive clones, the plasmid DNA with the inserts were extracted and sequenced for both directions using the primers SP6 and T7, based on the chemistry of Big Dye Terminator using an ABI Prism 3730 Genetic Analyser system.

3.5.3. Phylogenetic analysis of generated sequences

Manual verification of the chromatograms of 250 generated sequences was performed using Bellerophon (Huber et al., 2004). Fifty-one 51 *mcrA* clone sequences from Well D (4138–4141 m and 4659–4662 m) were found useful among a large number of sequenced clones. EMBOSS Transeq was used for the transformation of the sequences into respective protein sequences (Rice et al., 2000). These sequences were identified, characterised using the protein databases (GenBank/EMBL/PDB) and aligned with their best matches in the database in Clustal Ω (Madeira et al., 2019).

4. Results

4.1. Rock-Eval pyrolysis

The TOC content of the samples ranges from 0.13 to 0.70%, 0.11–1.61%, 0.13–1.28%, 0.13–2.27% and 0.05–1.33% in Well A, Well B, Well C-1, Well C-2 and Well D, respectively. The S_1 values range from 0.01 to 0.11 mg HC/g, 0.01–8.03 mg HC/g, 0.01–7.41 mg HC/g, 0.05–14.8 mg HC/g and 0.10–7.88 mg HC/g in samples from Well A, Well B, Well C-1, Well C-2 and Well D, respectively. The S_2 ranges from 0.08 to 0.47 mg HC/g, 0.02–2.01 mg HC/g, 0.07–1.8 mg HC/g, 0.09–3.07 mg HC/g and 0.13–2.04 mg HC/g in Well A, Well B, Well C-1, Well C-2 and Well D, respectively. The HI and OI vary from 9 to 176 mg HC/g TOC and 85–723 mg CO_2/g TOC, respectively. The Tmax values of Well A, Well C-1, Well C-2 and Well D samples vary uniformly from 294 to 436 °C, respectively. The Tmax of Well B samples varies between 299 °C and 609 °C. The results of the Rock-Eval pyrolysis are shown in Table 3.

Table 3
Results of Rock-Eval pyrolysis of the studied samples from the ONGC wells.

Well A							Well B						
Sampling interval (m)	S1	S2	Tmax (°C)	TOC (%)	HI	OI	Sampling interval (m)	S1	S2	Tmax (°C)	TOC (%)	HI	OI
655–660	0.04	0.47	428	0.70	67	173	1145–1150	0.15	0.58	421	0.73	79	192
760–765	0.02	0.22	430	0.37	59	227	1345–1350	0.34	0.42	300	0.33	127	245
805–810	0.02	0.14	423	0.24	58	308	1545–1550	0.05	0.20	423	0.22	91	350
860–865	0.02	0.08	417	0.13	62	400	1745–1750	0.18	0.30	417	0.21	143	357
900–905	0.02	0.11	418	0.26	42	308	1945–1950	8.03	2.01	299	1.28	157	88
960–965	0.02	0.11	428	0.16	69	469	2145–2150	0.07	0.12	436	0.13	92	285
1005–1010	0.02	0.11	423	0.25	44	264	2340–2345	1.01	0.59	304	0.40	148	200
1060–1065	0.02	0.28	427	0.46	61	178	2540–2545	2.41	1.05	299	0.64	164	155
1105–1110	0.02	0.12	430	0.27	44	244	2740–2745	0.90	0.47	423	0.34	138	174
1160–1165	0.01	0.08	432	0.24	33	225	2940–2945	0.44	0.27	421	0.19	142	200
1205–1210	0.03	0.14	424	0.30	47	313	3140–3145	0.56	0.27	410	0.24	112	200
1260–1265	0.03	0.12	432	0.26	46	258	3340–3345	0.33	0.27	416	0.16	169	312
1305–1310	0.02	0.13	421	0.25	52	192	3545–3550	0.33	0.25	417	0.16	156	350
1360–1365	0.02	0.12	428	0.17	71	388	3735–3740	0.01	0.02	609	0.23	9	126
1405–1410	0.02	0.10	422	0.18	56	400	3945–3950	0.50	0.36	300	0.37	97	200
1460–1465	0.02	0.22	430	0.38	58	174	4150–4155	0.26	0.40	433	0.33	121	215
1505–1510	0.02	0.13	425	0.22	59	250							
1560–1565	0.03	0.11	318	0.23	48	309							
1600–1605	0.02	0.08	318	0.14	57	464							
1660–1665	0.11	0.41	312	0.29	141	403							
1705–1710	0.09	0.28	313	0.28	100	268							
1725–1730	0.07	0.27	311	0.24	112	246							

Well C-1							Well C-2						
Sampling interval (m)	S1	S2	Tmax (°C)	TOC (%)	HI	OI	Sampling interval (m)	S1	S2	Tmax (°C)	TOC (%)	HI	OI
860–865	0.01	0.08	433	0.28	29	193	1805–1810	2.65	0.93	297	0.60	155	113
960–965	0.01	0.09	430	0.20	45	340	1900–1905	1.09	0.48	298	0.37	130	146
1055–1060	0.01	0.08	434	0.14	57	429	2000–2005	0.27	0.20	303	0.23	87	148
1145–1150	0.06	0.26	329	0.29	90	424	2100–2105	0.08	0.09	424	0.13	69	154
1245–1250	0.02	0.08	423	0.21	38	238	2200–2205	1.57	0.81	299	0.50	162	174
1360–1365	0.02	0.07	414	0.14	50	357	2300–2305	0.31	0.39	307	0.37	105	330
1460–1465	0.02	0.12	426	0.16	75	344	2400–2405	0.61	0.33	294	0.33	100	285
1560–1565	0.01	0.07	428	0.10	70	480	2500–2505	0.85	0.47	297	0.40	118	202
1660–1665	0.01	0.06	436	0.14	43	264	2605–2610	0.92	0.51	297	0.46	111	213
1760–1765	0.01	0.07	433	0.07	100	486	2700–2705	14.78	3.07	299	2.27	135	73
1865–1870	0.01	0.06	434	0.13	46	269	2800–2805	0.14	0.19	427	0.27	70	348
1960–1965	0.12	0.19	311	0.15	127	273	2900–2905	0.05	0.18	430	0.17	106	329
2060–2065	0.02	0.07	317	0.05	140	680							
2160–2165	0.04	0.10	429	0.16	62	294							
2260–2265	0.03	0.10	422	0.18	56	506							
2360–2365	0.15	0.18	390	0.26	69	723							
2460–2465	0.10	0.14	408	0.16	88	631							
2560–2565	7.32	1.80	298	1.33	135	139							
2660–2665	0.02	0.09	434	0.17	53	394							
2765–2770	0.02	0.07	429	0.14	50	550							
2860–2865	0.05	0.18	435	0.19	95	368							
2960–2965	0.01	0.08	433	0.17	47	488							
3095–3100	0.08	0.29	429	0.28	104	250							

	Well D				
Sampling interval (m)	S1	S2	Tmax (°C)	TOC (%)	HI	OI
3105–3110	0.10	0.13	425	0.11	118	355
3195–3200	0.96	0.72	301	0.41	176	202
3230–3235	0.44	0.45	304	0.32	141	222
3365–3370	0.97	0.57	304	0.44	130	182
3460–3465	0.51	0.37	302	0.33	112	224
3603–3608	4.07	1.38	296	0.83	166	98
3720–3723	1.20	0.76	304	0.57	133	198
3801–3804	2.45	1.05	300	0.70	150	169
3900–3903	6.57	1.67	297	1.17	143	87
4050–4053	2.74	1.06	298	0.79	134	157
4138–4141	7.62	1.90	298	1.35	141	107
4231–4234	0.50	0.32	306	0.36	89	272
4323–4326	1.49	0.70	302	0.65	108	192
4416–4419	1.62	0.77	302	0.86	90	217
4500–4503	1.82	0.93	301	0.61	152	161
4659–4662	7.88	2.04	302	1.61	127	85
4752–4755	3.39	1.23	300	0.80	154	108
4851–4854	3.42	1.31	303	1.07	122	134

(*continued on next page*)

Table 3 (*continued*)

Sampling interval (m)	Well D					
	S1	S2	Tmax (°C)	TOC (%)	HI	OI
4923–4926	2.93	1.17	305	0.95	123	145
4998–5001	2.41	0.98	301	0.94	104	138

4.2. Elemental and stable isotope ratio

The TOC/N (henceforth C/N) ratio (weight/weight) values are in the range 4–17, 5–25, 4–32, 4–41 and 5–34 in samples from Well A, Well B, Well C-1, Well C-2 and Well D, respectively (Table 4). The $\delta^{13}C$ values of samples from Well A, Well B, Well C-1, Well C-2 and Well D range from −25.6‰ to −23.7‰, −26.6‰ to −25.2‰, −26.4‰ to −21.7‰, −26.5‰ to −25.7‰ and −27‰ to −26.0‰, respectively (Table 4). The $\delta^{15}N$ values vary from 3.0‰ to 4.4‰, 3.5‰ to 4.6‰, 3.3‰ to 4.4‰, 3.5‰ to 4.0‰ and 3.5‰ to 4.5‰ in samples from Well A, Well B, Well C-1, Well C-2 and Well D, respectively. The values of $\delta^{13}C$, $\delta^{15}N$ and C/N ratios of Well A, Well B, Well C-1, Well C-2 and Well D, with respect to different geological ages, are given in Supplementary Table S1.

4.3. Aliphatic hydrocarbons

The GC–MS analysis shows the presence of *n*-alkanes (*n*-C_{14} to *n*-C_{35}) and isoprenoid alkanes (pristane and phytane) in samples from the studied wells except Well A, where the quantifiable presence of alkanes is not observed. The Well B, Well C-1 and Well C-2 samples show the unimodal distribution of *n*-alkanes with the prevalence of short-chain homologues (*n*-C_{19} and *n*-C_{20}). In contrast, samples from the Well D show unimodal distribution having dominant mid-chain (*n*-C_{21}, *n*-C_{22} and *n*-C_{23}) *n*-alkanes. Parameters such as Carbon Preference Index (CPI)

Table 4
C/N (w/w) ratio and stable isotope ratio of organic carbon and nitrogen of bulk OM of the samples from ONGC wells.

Well A				Well B				Well C-1			
Sampling interval (m)	C/N	$\delta^{13}C$ (‰)	$\delta^{15}N$ (‰)	Sampling interval (m)	C/N	$\delta^{13}C$ (‰)	$\delta^{15}N$ (‰)	Sampling interval (m)	C/N	$\delta^{13}C$ (‰)	$\delta^{15}N$ (‰)
655–660	17.3	–24.3	3.0	1145–1150	18.0	–26.8	3.6	860–865	6.1	–21.7	4.1
760–765	9.3	–24.3	4.4	1345–1350	8.4	–25.5	4.0	960–965	5.6	–21.7	4.4
805–810	7.1	–23.7	4.3	1545–1550	5.5	–25.2	4.6	1055–1060	5.2	–25.2	4.1
860–865	5.8	–23.9	4.4	1745–1750	6.8	–25.6	4.2	1145–1150	7.4	–24.7	4.2
900–905	6.8	–24.5	3.8	1945–1950	24.5	–26.6	3.9	1245–1250	4.8	–25.2	3.9
960–965	5.2	–24.1	4.1	2145–2150	6.2	–25.6	3.5	1360–1365	5.0	–25.4	4.0
1005–1010	5.3	–24.3	4.1	2340–2345	9.0	–26.3	3.8	1460–1465	5.0	–25.9	4.0
1060–1065	4.2	–24.9	3.8	2540–2545	13.3	–26.4	3.8	1560–1565	4.4	–25.8	3.9
1105–1110	6.4	–24.6	3.8	2740–2745	11.7	–26.4	3.8	1660–1665	5.1	–25.7	3.4
1160–1165	5.2	–25.0	4.1	2940–2945	7.4	–26.5	3.8	1760–1765	5.2	–25.6	3.7
1205–1210	5.9	–24.8	4.0	3140–3145	9.2	–26.6	3.6	1865–1870	5.5	–25.8	3.6
1260–1265	6.7	–24.8	3.7	3340–3345	6.6	–26.3	3.7	1960–1965	6.2	–26.0	3.5
1305–1310	7.5	–24.8	3.6	3545–3550	13.9	–26.4	3.9	2060–2065	4.9	–25.7	3.3
1360–1365	5.0	–25.2	4.0	3735–3740	10.6	–25.5	4.5	2160–2165	6.0	–25.7	3.6
1405–1410	7.2	–25.6	3.8	3945–3950	6.9	–25.3	4.2	2260–2265	5.3	–26.2	3.7
1460–1465	6.2	–25.2	3.9	4150–4155	7.8	–25.4	4.4	2360–2365	10.3	–26.0	4.0
1505–1510	6.1	–25.3	4.0					2460–2465	6.8	–26.2	3.8
1560–1565	5.2	–25.6	3.6					2560–2565	31.6	–26.3	3.6
1600–1605	6.7	–24.7	4.0					2660–2665	5.8	–26.1	3.8
1660–1665	5.8	–24.9	3.7					2765–2770	5.2	–26.2	3.6
1705–1710	5.4	–25.0	3.8					2860–2865	5.1	–26.4	3.8
1725–1730	5.2	–25.0	4.2					2960–2965	4.7	–26.0	3.7
								3095–3100	5.4	–25.6	4.0

Well C-2				Well D			
Sampling interval (m)	C/N	$\delta^{13}C$(‰)	$\delta^{15}N$(‰)	Sampling interval (m)	C/N	$\delta^{13}C$(‰)	$\delta^{15}N$(‰)
1805–1810	16.4	–26.5	3.5	3105–3110	5.4	–26.0	4.2
1900–1905	8.4	–26.5	3.7	3195–3200	7.7	–26.2	3.9
2000–2005	6.4	–26.2	3.5	3230–3235	6.5	–26.0	4.0
2100–2105	5.5	–25.7	3.6	3365–3370	9.3	–26.4	3.5
2200–2205	9.9	–26.5	3.9	3460–3465	6.8	–26.0	3.9
2300–2305	8.6	–26.0	3.6	3603–3608	16.7	–26.7	3.6
2400–2405	9.9	–26.1	3.7	3720–3723	9.9	–26.3	3.5
2500–2505	9.4	–26.5	3.9	3801–3804	15.6	–26.6	3.5
2605–2610	10.0	–26.4	4.0	3900–3903	23.0	–27.0	3.5
2700–2705	41.2	–26.3	3.6	4050–4053	15.7	–26.8	3.7
2800–2805	6.1	–26.3	3.9	4138–4141	24.2	–26.9	3.7
2900–2905	4.9	–26.1	4.0	4231–4234	9.1	–26.3	3.8
				4323–4326	13.8	–26.8	4.1
				4416–4419	11.9	–26.9	3.9
				4500–4503	11.6	–26.7	4.5
				4659–4662	34.0	–27.0	3.8
				4752–4755	14.9	–26.8	4.5
				4851–4854	19.2	–26.7	4.2
				4923–4926	16.2	–26.8	3.9
				4998–5001	15.4	–26.8	4.3

for short-chain alkane (CPI-1) and long-chain *n*-alkanes (CPI-2) are used for interpreting the source of the OM. The studied samples show that the CPI-1 and CPI-2 values range from 0.90 to 1.50 and 0.80 to 1.20 (Table 5; Supplementary Table S2). The aquatic macrophyte (plant) *n*-alkane proxy (P_{aq}) values lie between 0.8 and 0.9 (Table 5). The pristane/phytane (Pr/Ph) ratio values of samples from Well B, Well C-1 and Well C-2 are < 1, although in Well D samples, the ratio range between 1 and 4.7 (Table 5). pristane/C_{17} (Pr/C_{17}) and phytane/C_{18} (Ph/C_{18}) values range from 0.77–4.28 to 0.45–2.16, respectively (Table 5).

4.4. Clone library analysis

The neighbour-joining method, which is based on the Jones-Taylor-Thompson model (Saitou and Nei, 1987; Jones et al., 1992), was used for constructing the alignment file in MEGA version 7.0 (Fig. 3; Kumar et al., 2016). Both clone libraries have very low diversity and abundance, and the dendrogram shows that the clones from the present study are grouped into a separate clade. The nucleotide sequences of the *mcrA* clones were submitted to GenBank, and the clones from Well D have accession numbers MT339340 to MT339390 (51 clones).

5. Discussion

5.1. Kerogen maturity and type

TOC values > 1% in seven (four samples from Well D, one sample from Well B, one sample from Well C-1 and one sample from Well C-2; Table 3) out of 93 samples, fall in the fair hydrocarbon sources field in the HI/TOC plot (Fig. 4). With an average geothermal gradient of 27.6 °C km^{-1} (Akbar, 2011), it is likely that the deeper samples of these wells have reached the catagenesis phase and are likely to reflect cracking processes, but the shallower samples lie close to the diagenesis-catagenesis boundary and are unlikely to show any effect of thermal alteration. Low Tmax values (297–303 °C; Table 3) indicate immature kerogen and insignificant generation of hydrocarbon from these samples. The rest of the samples lie in the poor source sector of the HI/TOC plot (Fig. 4).

The kerogen type provides information about the origin, diagenesis and maturity of the OM (e.g., Peters, 1986; Boreham and Powell, 1993; Littke and Leythaeuser, 1993). The HI/OI plot (Fig. 5a) indicates the presence of Type III (gas prone) kerogen in the studied samples (Tissot and Welte, 1984; Laier et al., 1992). The HI/Tmax plot (Fig. 5b) indicates mostly immature nature of the samples, and the plot is consistent with the presence of Type III and Type IV kerogen in the samples. Those samples with TOC > 1%, fall within the immature Type III kerogen zone in Fig. 5b. Similarly, the presence of Type III containing immature OM (TOC = 0.2–0.6%) is reported in the Miocene Bengal Basin (Foredeep) sediments in Bangladesh (Shamsuddin and Khan, 1991).

5.2. Sources and depositional environments of OM

5.2.1. Interpretations based on stable isotope signatures

The C/N ratio of the Well A, Well B, Well C-1, Well C-2 and Well D samples range from 4–17, 5–25, 4–32, 5–41 and 5–34, respectively (Table 4), indicating mixed freshwater algae (C/N ratio 6–8) and terrestrial plants (C/N > 15) derived OM source (Meyers, 1994). An increase in the C/N ratio with depth is likely mediated by an increase in TOC values instead of selective removal of N and indicate a change in OM source from freshwater phytoplankton during Pliocene and Pleistocene to C_3 plants growing in marshy depositional settings during Miocene (Fig. 6a,b). The $\delta^{13}C$ composition coupled with the C/N ratio is further used to delineate the sources of OM, especially to identify the relative contribution from aquatic versus terrestrial sources (Das et al., 2008; Ramaswamy et al., 2008; Cai et al., 2015; Careddu et al., 2015; Li et al., 2016). The $\delta^{13}C$ vs C/N plot (Fig. 7a) of the studied samples indicates a primarily freshwater phytoplankton and C_3 terrestrial plant/freshwater macroalgal source of OM (Cerling and Harris, 1999; Diefendorf et al., 2010; Kohn, 2010; Cernusak et al., 2013). The presence of

Table 5
Alkane parameters of the studied samples from the ONGC wells. The Well A samples do not yield any measurable amount of alkanes. Samples of the Well D, showing the presence of methanogenic archaea, are marked in bold.

Well Name	Sampling interval (m)	CPI-1	CPI-2	TAR	P_{aq}	Pr/Ph	Pr/C_{17}	Ph/C_{18}	(Pr + C_{17})/(Ph + C_{18})
	1145–1150	1.40	1.20	0.57	0.92	0.85	3.38	1.89	0.72
Well B	1945–1950	1.50	0.90	0.09	0.95	0.40	3.27	2.16	0.36
	2540–2545	0.90	0.90	0.15	0.92	0.81	2.52	1.38	0.66
	3545–3550	1.20	0.80	0.32	0.88	0.70	2.42	1.45	0.59
Well C-1	2560–2565	1.50	1.20	0.26	0.88	0.32	0.93	0.82	0.30
	1805–1810	1.00	1.00	0.29	0.91	0.46	1.41	1.64	0.49
Well C-2	2200–2205	1.10	0.80	0.22	0.91	0.65	1.67	1.37	0.60
	2700–2705	1.10	1.10	0.27	0.87	0.58	1.32	0.86	0.47
	3603–3608	1.10	1.20	0.34	0.91	2.03	2.43	0.73	1.21
	3720–3723	1.10	1.20	0.33	0.90	2.28	4.19	1.20	1.54
	3801–3804	1.10	1.10	0.34	0.90	1.70	2.63	1.03	1.19
	3900–3903	1.10	1.10	0.24	0.90	2.08	1.46	0.55	1.24
	4050–4053	0.90	1.20	0.29	0.91	1.53	2.19	0.97	1.09
	4138–4141	**1.40**	**1.20**	**0.22**	**0.91**	**1.02**	**0.77**	**0.70**	**0.97**
Well D	4323–4326	1.10	1.10	0.88	0.79	2.20	4.28	1.15	1.45
	4416–4419	1.10	1.20	0.57	0.83	2.53	3.05	0.73	1.42
	4500–4503	1.10	1.10	0.57	0.80	2.32	3.95	0.98	1.44
	4659–4662	**1.10**	**1.10**	**0.92**	**0.81**	**3.26**	**3.74**	**0.57**	**1.51**
	4752–4755	1.00	1.10	0.24	0.82	2.51	1.99	0.67	1.51
	4851–4854	1.20	1.10	0.51	0.79	4.73	2.48	0.45	2.07
	4923–4926	1.20	1.20	0.58	0.84	2.76	4.12	0.88	1.60
	4998–5001	0.90	1.10	0.60	0.82	2.98	3.05	0.74	1.69

CPI-1 = $1/2 \times (((C_{15} + C_{17} + C_{19})/(C_{14} + C_{16} + C_{18})) + ((C_{15} + C_{17} + C_{19}))/(C_{16} + C_{18} + C_{20})))$.
CPI-2 = $1/2\times(((C_{25} + C_{27} + C_{29} + C_{31} + C_{33})/(C_{24} + C_{26} + C_{28} + C_{30} + C_{32})) + ((C_{25} + C_{27} + C_{29} + C_{31} + C_{33})/(C_{26} + C_{28} + C_{30} + C_{32} + C_{34})))$.
$P_{aq} = (C_{23} + C_{25})/(C_{23} + C_{25} + C_{29} + C_{31})$.
Pristane/phytane ratio = Pr/Ph.
TAR = $(C_{27} + C_{29} + C_{31})/ (C_{15} + C_{17} + C_{19})$.

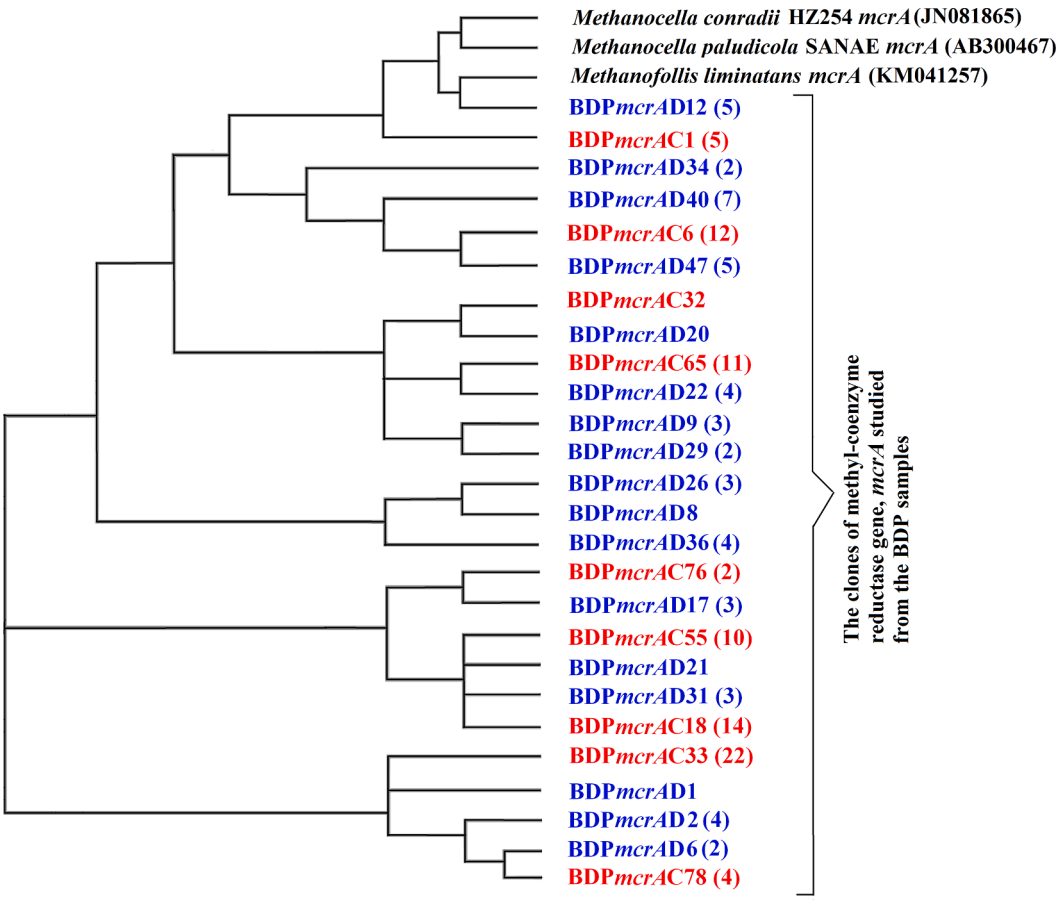

Fig. 3. Neighbour-joining phylogenetic tree of amino acid sequences of generated *mcrA* clone sequences. The tree is unrooted, and the clones from Well D (4138–4141 m and 4659–4662 m) are in blue. The number in parenthesis indicates the copy number of the clones retrieved.

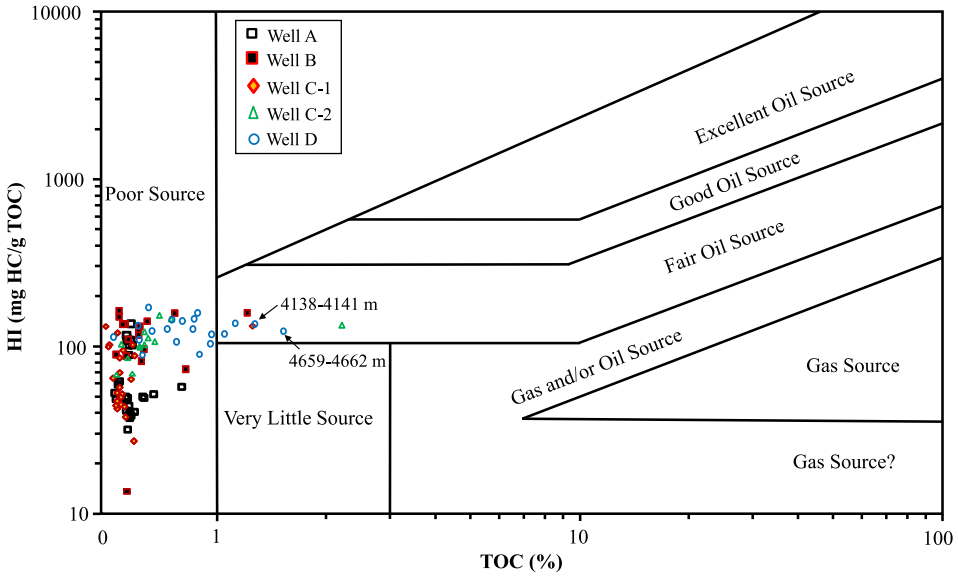

Fig. 4. Relationship between HI and TOC in the studied samples.

Type III kerogen in these samples is consistent with our observation because kerogen type does not discriminate between terrestrial higher plant and freshwater aquatic plant-derived sources of OM. Our observation matches with the reported presence of terrestrial (humic) OM in the Bengal Basin (Bengal Foredeep) sediments as described by Shamsuddin and Khan (1991), who used the $\delta^{13}C$ composition of hydrocarbon gases to postulate the source of the sedimentary OM. The $\delta^{13}C$ vs C/N plot may also indicate specific depositional environments such as tidal flats, C_3 marsh and brackish transition zones (Khan et al., 2015). The studied samples mostly fall in the tidal flat and C_3 marsh zone, as indicated by the $\delta^{13}C$ vs C/N plot (Fig. 7b). A gradual change in the OM source from aquatic (Pleisto-Pliocene) to terrestrial C_3 plant (Miocene)

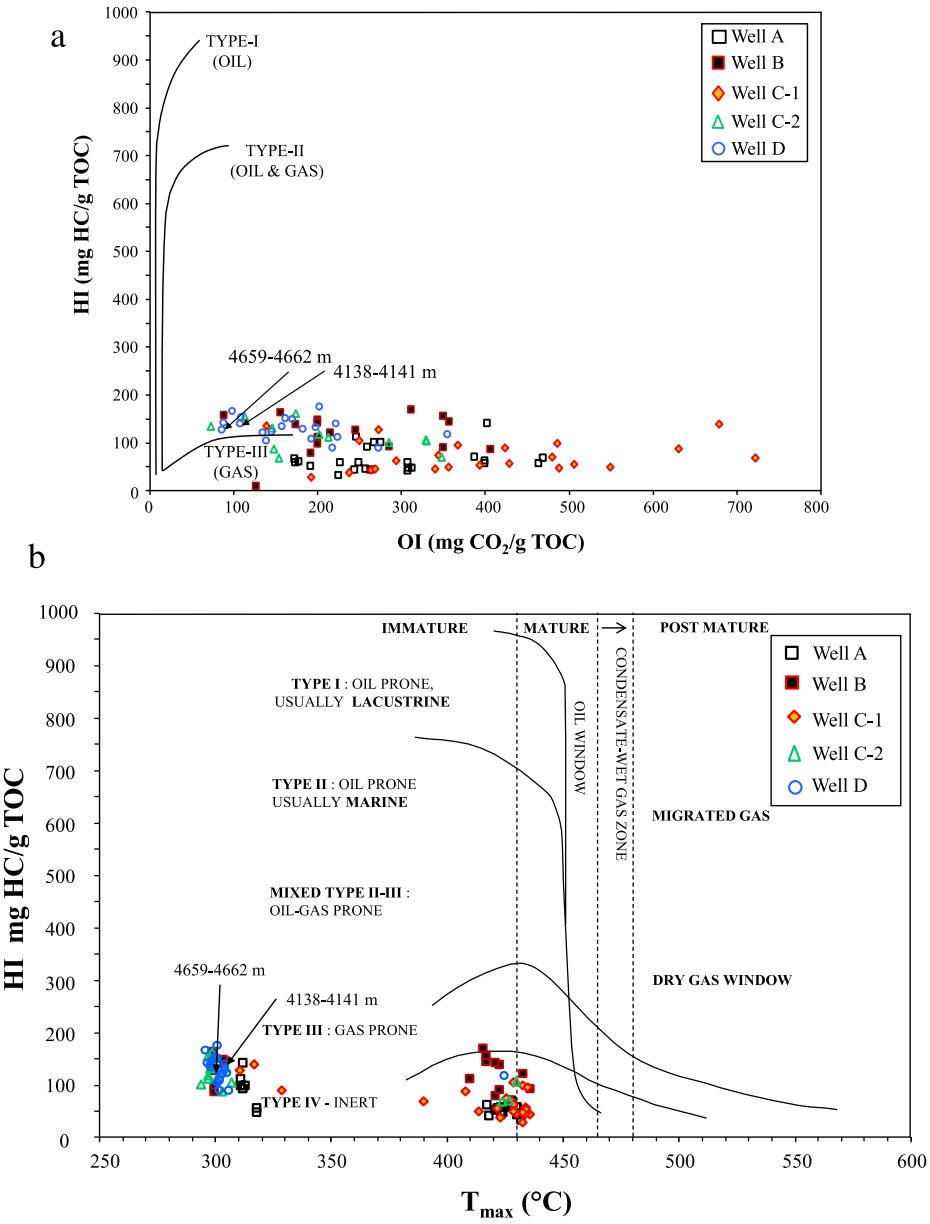

Fig. 5. Relationship between: (a) HI and OI, and (b) HI and Tmax.

and from tidal flat (Pleisto-Pliocene) to C_3 marsh (Miocene) depositional environments with age is also evident in the $\delta^{13}C$ vs C/N plots (Fig. 8a, b).

The absence of C_4 plant-derived OM in the studied Bengal Basin sediments, despite the reported presence of C_4 plants in the Lower Ganga Plain (Basu et al., 2015), may result from the low preservation potential of OM derived from the C_4 plants (Wynn and Bird, 2007). Two Well C-1 samples having depth intervals of 860–865 m and 960–965 m show slightly more enriched $\delta^{13}C$ values (−21.8‰ and −21.7‰, respectively), indicating a blend of C_3 and C_4 plant-derived OM (Fig. 6c). More enriched $\delta^{13}C$ values in Pleistocene sediments of the Bengal Basin are consistent with the reported presence of C_4 plant-derived OM in Bengal Fan sediments, which shows a more enriched signature during the Pleistocene, although the reported appearance of C_4 plant-derived organic matter has been noticed in lower Bengal Fan sediments since the Miocene (France-Lanord and Derry, 1994; Galy et al., 2010). The absence of a mixed C_3-C_4 signal in Miocene Bengal Basin sediments may further be explained in light of possible lower abundance of C_4 plants in marginal marine environments.

Early diagenesis and post-depositional decomposition of OM primarily affect the C/N ratio (e.g., Walker and McComb, 1985). The stable isotope signature is considered resistant to isotopic alteration during post-depositional diagenesis (Schelske and Hodell, 1995; Teranes and Bernasconi, 2000; Kemp et al., 2012), although selective preservation of ^{13}C-depleted compounds under oxic environments (Lehmann et al., 2002) and ^{15}N enrichment in residual OM is reported (Middelburg and Herman, 2007). The influence of decomposition on the $\delta^{13}C$ value depends on the type of OM, whereas the effect on $\delta^{15}N$ is primarily microbially controlled (Galman et al., 2009). In the studied Bengal Basin sediments, an insignificant correlation ($R^2 < 0.4$) between C/N and $\delta^{13}C$ (except Well D) and between C/N and $\delta^{15}N$ ($R^2 < 0.3$) indicates that the stable isotope signature of the sedimentary OM is not significantly affected by bacterial decomposition (Fig. 9a,b). On the contrary, the good correlation ($R^2 = 0.6$) between C/N and $\delta^{13}C$ in the Well D samples indicates significant bacterial activity.

The $\delta^{15}N$ values of the studied samples, which range between 3‰ and 5‰, lie above the range of atmospheric N_2-fixation and likely indicate an OM derived from C_3 marsh plants. The $\delta^{15}N$ signature of C_3

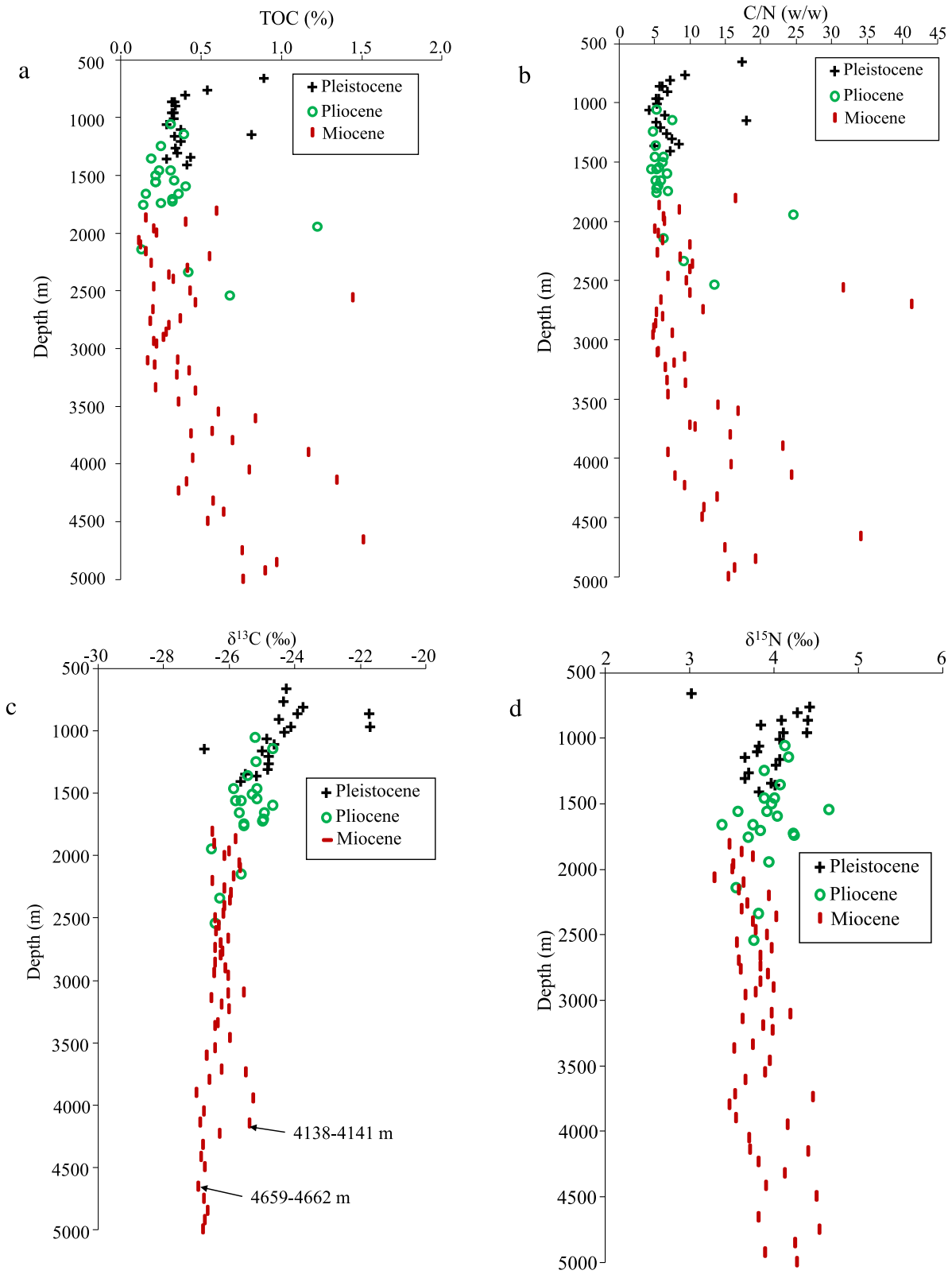

Fig. 6. Variation of (a) TOC%, (b) C/N (w/w), (c) $\delta^{13}C$ and (d) $\delta^{15}N$ with age.

marsh plants, such as mangroves, is generally higher than terrestrial plants (Kuramoto and Minagawa, 2001). Selective loss of ^{14}N through denitrification, occurring at the sediment–water interface, and selective removal of diagenetically sensitive amino acids under oxic conditions (Nguyen and Harvey, 1997; Möbius et al., 2010) may further contribute to the heavier $\delta^{15}N$ values (Natelhoffer and Fry, 1988; Högberg, 1990; Kuramoto and Minagawa, 2001; Bedard-Haughn et al., 2003). We did not observe a systematic change in $\delta^{15}N$ values with depth (Fig. 6d), although an increase in $\delta^{15}N$ values due to microbial decomposition with depth is often observed (Billings and Richter, 2006; Craine et al.,

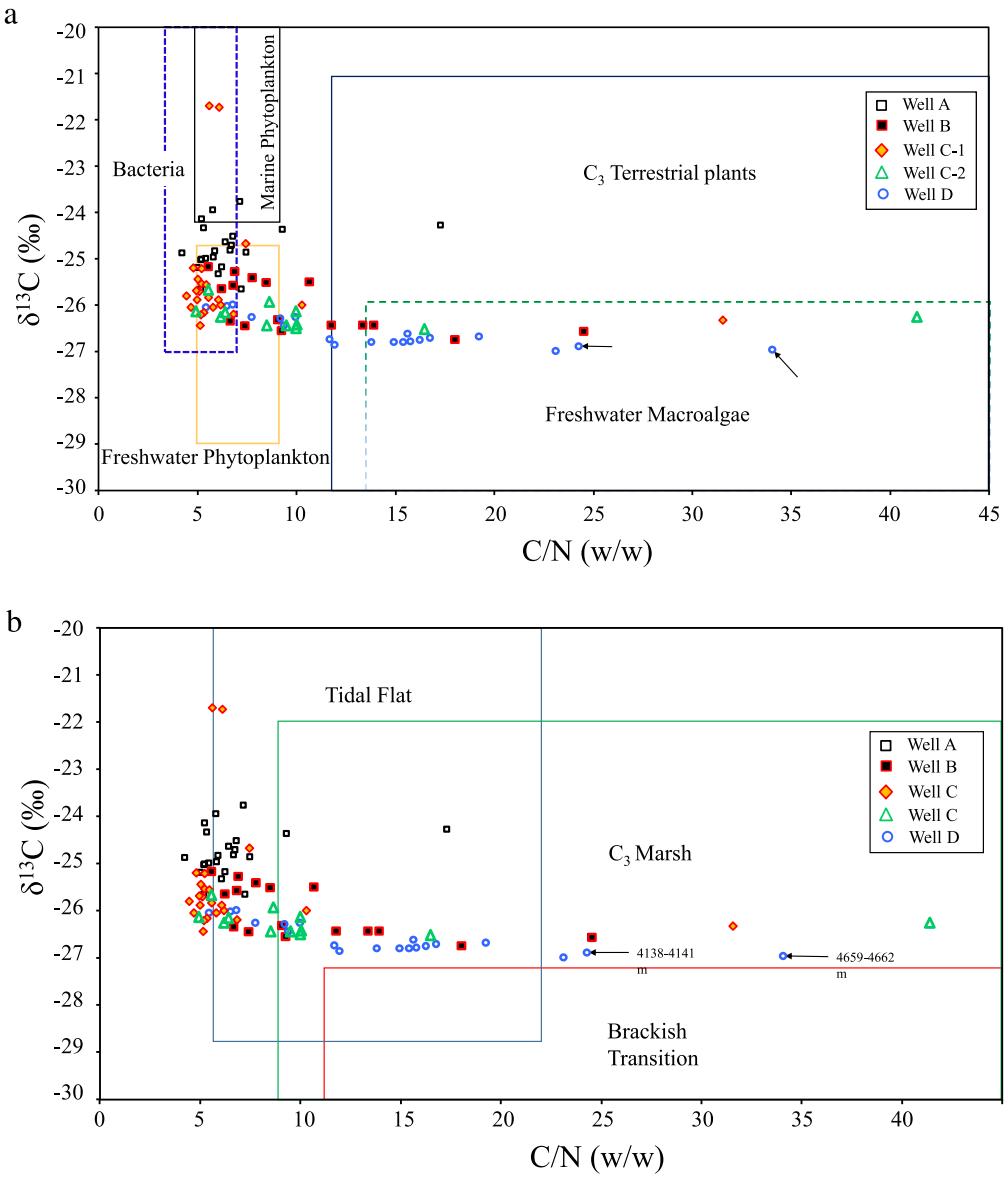

Fig. 7. $\delta^{13}C$ and C/N plot showing: (a) the sources of OM and (b) depositional environments of the samples.

2015). This may not imply an absence of diagenetic effects, but rather that the sedimentary OM is mostly resistant to further degradation, and less sensitive to post-depositional diagenetic changes.

5.2.2. Alkane based interpretation of the sources and depositional environments of OM

GC–MS analysis shows the presence of *n*-alkanes (*n*-$C_{14–35}$) and isoprenoid alkanes (pristane and phytane) in samples from Well D, Well C-1, Well C-2 and Well B (Table 5). The absence of a measurable amount of alkanes in the Well A samples may result from low TOC content (Table 3). Phytoplankton and algae primarily produce short-chain *n*-alkanes (*n*-C_{14} to *n*-C_{24}), enriched in *n*-$C_{15,17,19}$ with dominant *n*-C_{17} alkane, and show a strong odd over even carbon preference (Meyers and Ishiwatari, 1993; Meyers, 1997; Sakata et al., 1997; Meyers and Teranes, 2001). Microbial activity (also fossil fuel input) contributes to the short-chain *n*-alkanes without any strong odd over even carbon number preference (Bouloubassi et al., 1998). Terrestrial higher (vascular) plants produce long-chain *n*-alkanes (*n*-C_{25} to *n*-C_{35}) enriched in *n*-$C_{27,29,31}$ alkanes with a strong odd-to-even carbon preference (Eglinton and Hamilton, 1967). In some instances, long-chain *n*-alkanes are linked to phytoplankton and microbial sources, but an odd over even carbon preference is not observed (Volkman et al., 1998). Aquatic plants, including floating and submerged species, are characterised by *n*-$C_{21,23,25}$ alkanes (Meyers and Teranes, 2001).

The CPI takes into account the relative abundance of odd vs even *n*-alkanes and indicates the source of the immature sedimentary OM (Bush and McInerney, 2013). Terrestrial higher plants typically show high (> 5) CPI-2 ($CPI_{25–35}$) values with strong odd-to-even carbon preference (Eglinton and Hamilton, 1967; Rieley et al., 1991; Bouloubassi et al., 1998). On the contrary, phytoplankton and aquatic plant-derived OM exhibits CPI-1 ($CPI_{15–19}$) values close to unity (Tareq et al., 2005; Jeng, 2006). Long-chain *n*-alkanes derived from marine phytoplankton, microorganisms and hydrocarbon generally do not have an odd-to-even carbon preference (Volkman et al., 1998). Near-unity CPI-1 (1.0–1.6) and CPI-2 (0.8–1.0) values indicate the absence of strong odd-even carbon preference and primarily an aquatic source of OM (Table 5; Fig. 10a,b). CPI values close to 1.0 may also result from microbial activity or thermal alteration of kerogen (Xing et al., 2011). The measurable presence of methanogenic archaea only in two Miocene sediments (discussed below) does not support extensive microbial activity. Instead, a geothermal gradient of ~27–28 °C km^{-1} in Bengal Basin (Akbar (2011) implies the onset of thermal maturity of deeper Miocene

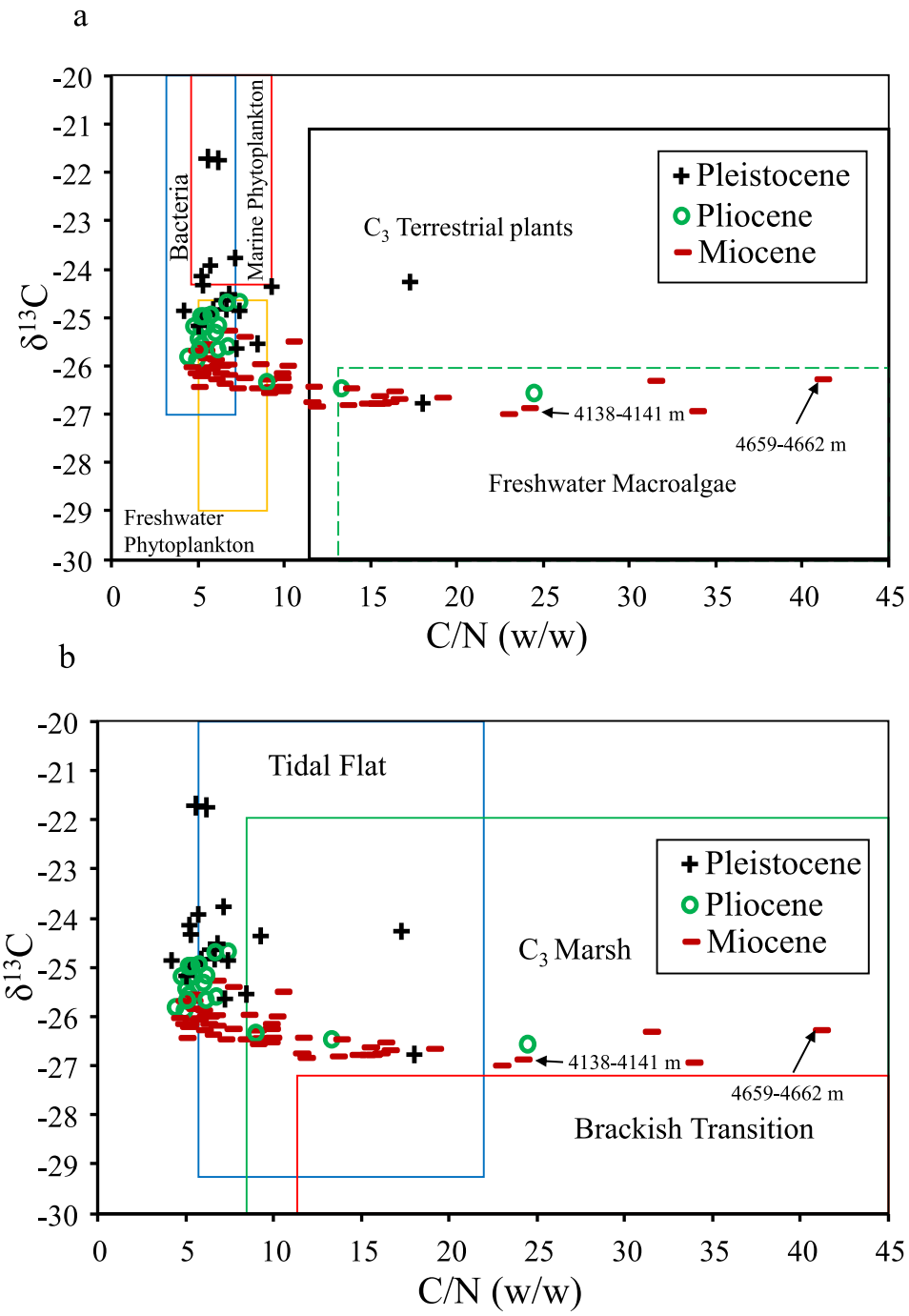

Fig. 8. $\delta^{13}C$ and C/N plot showing: (a) the sources of OM and (b) depositional environments of the samples with age.

sediments. Our observation is supported by terrigenous to aquatic ratio (TAR) values < 1 (Table 5) of the studied samples (Bourbonniere and Meyers, 1996; Silliman et al., 1996; Ortiz et al., 2013). An increase in TAR values with depth indicates a change in the source of OM from aquatic (during Pliocene and Pleistocene) to terrestrial (Miocene) (Fig. 10c).

P_{aq} is used to determinate the relative contribution of terrestrial plants (P_{aq} < 0.1), emergent aquatic plants (P_{aq} = 0.1–0.4) and non-emergent (submerged and floating) aquatic plants (P_{aq} = 0.4–1.0) to the sedimentary OM (Ficken et al., 2000). The P_{aq} (0.8–0.9) values of the studied samples (Table 5) indicate a primarily non-emergent aquatic plant source of the sedimentary OM. Our interpretation based on the CPI, TAR, P_{aq} values is consistent with the source interpretation based on the Rock-Eval pyrolysis, elemental C/N ratio and stable isotope data (Figs. 5 and 7).

Pristane (Pr) and phytane (Ph) are diagenetic products formed by oxidation and reduction of phytol, the side chain of chlorophyll-*a*. The pristane/phytane (Pr/Ph) ratio is used to determine the source of OM and paleodepositional and palaeo-redox interpretations (Didyk et al., 1978; Peters et al., 2005). High (> 3.0) Pr/Ph ratio in rock samples indicate terrigenous plant-derived OM input and deposition under oxic conditions, whereas a low (< 0.8) Pr/Ph ratio indicates anoxic, mostly saline to hypersaline, paleodepositional conditions associated with evaporites and carbonates (Peters et al., 2005). Pr/Ph values < 1 (Table 5) in the Well B, Well C-1 and Well C-2 samples and relatively low Pr/Ph ratio (mostly 1–3) in the Well D samples indicate non-terrestrial OM source and suggest deposition under variable, anoxic to oxic conditions.

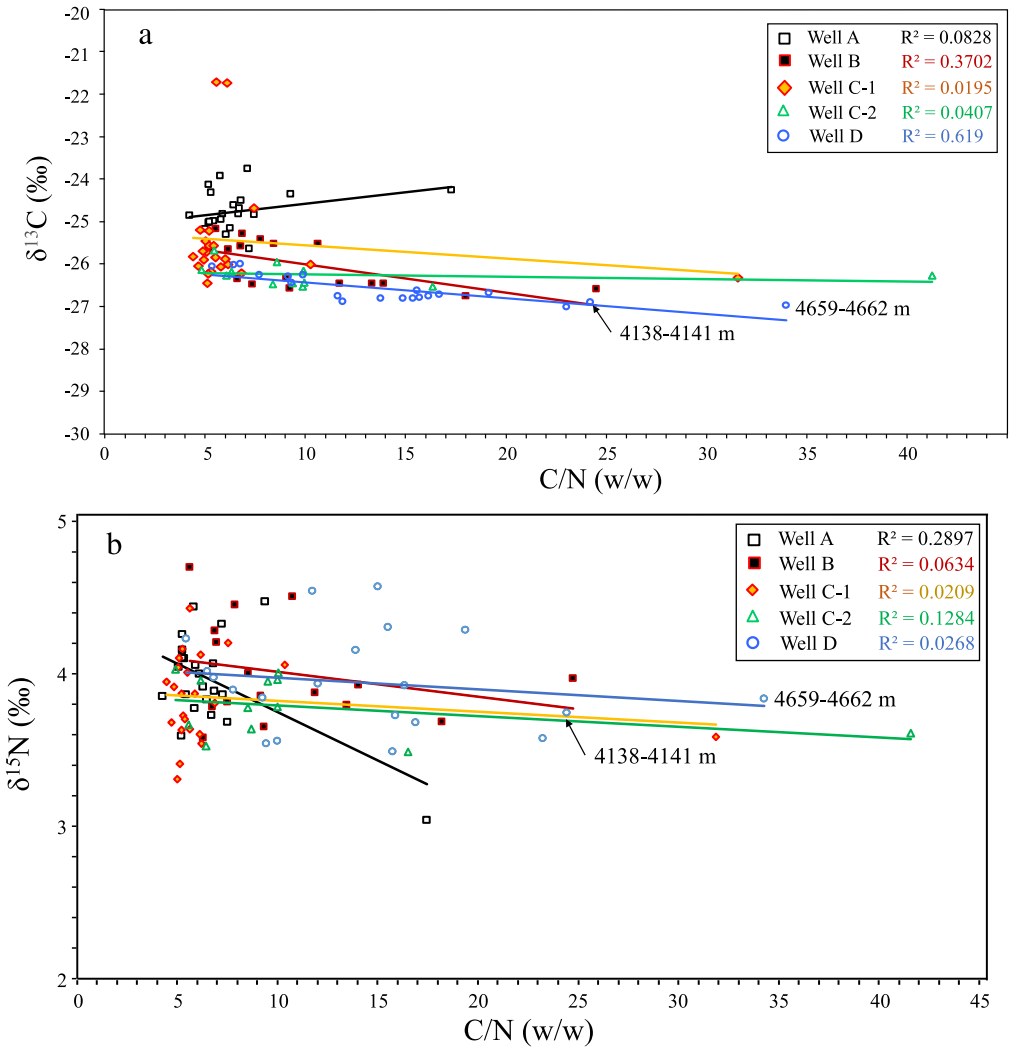

Fig. 9. (a) $\delta^{13}C$ vs C/N and (b) $\delta^{15}N$ vs C/N plots (R^2 values are indicated).

Notably, ten Haven et al. (1987) have advised against drawing conclusions on the paleoredox depositional conditions solely from the Pr/Ph ratio and assigned low Pr/Ph ratio (< 1) to hypersaline environments. In line with this, Peters et al. (2005) do not recommend Pr/Ph ratios in the range of 0.8–3.0 for interpreting paleoenvironmental conditions without corroborating data. Hence, we use Pr/*n*-C_{17} vs Ph/*n*-C_{18} cross plot for paleodepositional interpretation (Lijmbach, 1975). An oxic and terrestrial depositional settings are postulated from the Pr/*n*-C_{17} vs Ph/*n*-C_{18} cross plot (Fig. 11), except for one sample from the Well D (4138–4141 m) and samples from the Well C-1 and Well C-2 that fall in the suboxic zone of deposition (Fig. 11). Interestingly, none of our samples falls in reducing marine depositional conditions. Our observation is consistent with the reported immature nature of OM, postulated from higher Pr/*n*-C_{17} (2.7–5.6) and Pr/Ph ratios of the hydrocarbons (condensates), in the Bengal Foredeep region in Bangladesh (Shamsuddin and Khan, 1991).

The Pr/*n*-C_{17} and Ph/*n*-C_{18} ratios (Peters et al., 1995, 1999) further indicate the degree of biodegradation of the OM. The Pr/*n*-C_{17} and Ph/*n*-C_{18} ratios increase with an increased microbial decomposition of OM during biodegradation due to selective loss of *n*-alkanes compared to the isoprenoid alkanes (Peters et al., 1999). We use the (Pr + *n*-C_{17})/(Ph + *n*-C_{18}) ratio to study biodegradation because the effect of variation of any one variable is less on the ratio (Alexander et al., 1981; Das et al., 2009). Above or near unity (Pr + *n*-C_{17})/(Ph + *n*-C_{18}) ratio values indicate biodegradation in deeper Miocene sediments from Well D, including intervals (4138–4141 m and 4659–4662 m) (Table 5), which show the presence of methanogenic archaea (discussed below). Samples at these depths were likely thermally altered (considering a geothermal gradient of 27.6 °C km^{-1}). The use of (Pr + *n*-C_{17})/(Ph + *n*-C_{18}) ratio was based on the assumption that the isoprenoids result from degradation of the phytol side-chain of chlorophyll-*a*. However, pristane and phytane could be derived from thermally altered sedimentary organic matter containing isoprenoid components of archaeal lipids (Li et al., 1995; Rontani and Bonin, 2011). It is possible that the biodegradation reflected by the (Pr + *n*-C_{17})/(Ph + *n*-C_{18}) ratio was influenced by the isoprenoids released from the archaeal lipids during catagenesis.

5.3. Phylogenetic diversity

Methanogenic prokaryotes predominantly thrive in environments where sulphate reduction processes are not dominant. This is because oxido-reductive products of sulfur restrict methanogenesis (Oremland and Polcin, 1982). Hence, an attempt is made to trace the occurrence of sulfur oxidation and sulphate reduction processes that may affect the methane-producing prokaryotic population. In order to do so, the extracted environmental DNA samples are examined by characterising the *aprA* gene from the environmental DNA pool. The *aprA* gene encodes a subunit of the enzyme dissimilatory adenosine-5′-phosphosulphate reductase, which is primarily responsible for microbial sulfur oxidation and sulphate reduction and is highly conserved among sulfur-oxidising

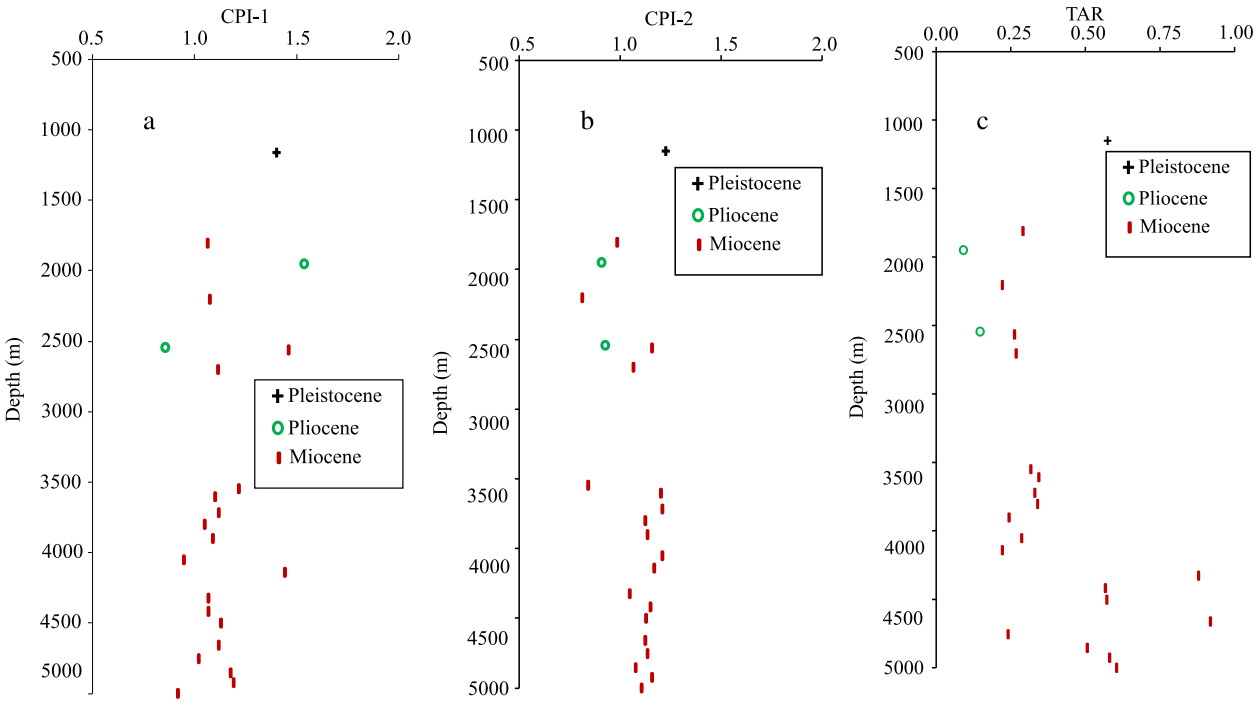

Fig. 10. Variation of (a) CPI-1, (b) CPI-2 and TAR values with age.

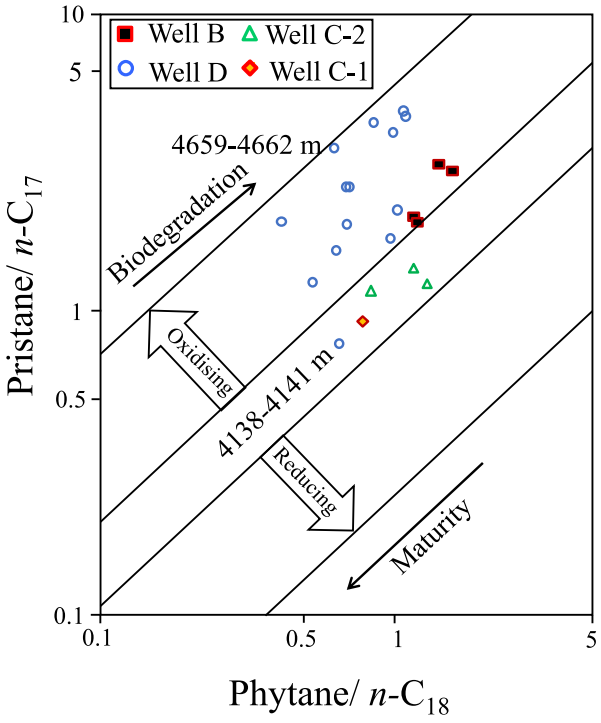

Fig. 11. Phytane/*n*-C_{18} vs pristane/*n*-C_{17} cross-plot (after Tewari et al., 2017) of the Bengal Basin samples recovered by the ONGC in West Bengal, India. Measurable *n*-alkanes were not detected in Well A.

and sulphate reducing prokaryotes. Hence it is frequently used as a tool in molecular phylogeny to identify the presence of sulfur-oxidising and sulphate-reducing prokaryotes (Meyer and Kuever, 2007). The studied samples show non-amplification during *aprA* PCR reaction, indicating no traces of any sulfur oxidising and sulphate-reducing prokaryotes in the studied samples.

The enzyme methyl co-enzyme reductase reduces the coenzyme-M bound methyl group and subsequently releases methane (Luton et al., 2002). This unique enzyme is ubiquitous in all methanogenic prokaryotes and is used as a tool for studying the molecular phylogeny of methanogens (Thauer, 1998).

The presence of *mcrA* and *aprA* genes was tested in Well D samples because Well D samples indicated significant bacterial activity. The amplification of the *mcrA* gene was achieved only in two Well D (4138–4141 m and 4659–4662 m) samples. A low diversity of methanogenic archaea was detected, and two dominant genera, *Methanocella* sp. and *Methanoformis* sp., are found in both the above-mentioned samples (Fig. 3). *Methanocella* has been reported as a hydrogenotrophic methanogen isolated from paddy field sediment (Sakai et al., 2010). The presence of methanogenic archaea indicates active biogenic methane generation at these depths in Well D (4138–4141 m and 4659–4662 m). Methanogenic archaea (*Methanocella* sp. and *Methanoformis* sp.) reported in the two Well D samples belong to hyperthermophilic groups (Mauerhofer et al., 2021) and could thrive well within the temperature ranges estimated from an average geothermal gradient of 27.6 °C km^{-1} in the Bengal Basin (Akbar, 2011).

The non-detection of prokaryotic methanogenesis gene signatures in the rest of the samples could possibly result from an absence of labile OM and/or unfavourable substrate conditions. At low TOC values, the cell growth and biomass accumulation could be lower than detection limits. Loss of cell abundance/biomass during storage is unlikely to affect the results because of the long shelf life of DNA. Interestingly, TOC values > 1% were mostly measured in deeper (> 2500 m) samples (Table 3), and both the two samples from Well D with methanogenic prokaryotes were retrieved below 4000 m depth (Table 2). Moreover, the clones from the Bengal Basin form a separate clade (or can be seen as a separate branch) in the phylogenetic tree (Fig. 3). Such in-grouping indicates that the Bengal Basin clones are functionally and phylogenetically distant from methanogenic archaea such as *Methanocella* sp. (Sakai et al., 2010). Further, it can be said that the methanogens growing in the deep Bengal Basin sediments are rare occurrences. For the convenience of data interpretations, the *mcrA* clones in two Well D samples are marked in Fig. 3.

Interestingly, the OM source of the two Well D samples, which show the presence of methanogenic archaea, is C_3 freshwater macroalgae

deposited under C_3 marshy conditions. Freshwater algae are associated with aliphatic and peptide-like labile compounds that may facilitate active methanogenesis (del Giorgio and Davis, 2003; Kellerman et al., 2018; Berberich et al., 2020). Enhanced methane production has been observed in OM derived from aquatic plants (Yakimovich et al., 2018), and experimental studies show higher methanogenic activities in sediments containing freshwater OM (Berberich et al., 2020; Yakimovich et al., 2020), although little published literature, exploring the effects of OM type on methanogens, exists.

6. Conclusions

The C/N and stable isotope ratios indicate primarily aquatic and C_3 plant sources of the OM, and sediment deposition under tidal flat and marshy environments. The *n*-alkane distribution (CPI, TAR and P_{aq}) in the studied samples agrees with the aquatic and C_3 terrestrial plant sources of the OM. A gradual change in the dominant OM source and depositional environments from Pleisto-Pliocene (aquatic; tidal flat) to Miocene (terrestrial C_3 plant; marsh) is evidenced in the $\delta^{13}C$ vs C/N plots and TAR values. Isoprenoid alkane distribution (Pr/Ph, Pr/*n*-C_{17} vs Ph/*n*-C_{18}) is consistent with a primarily non-marine aquatic plant source of the OM and indicates a terrestrial oxic depositional environment.

Kerogen maturity parameters, including Tmax, HI, OI and TOC, indicate an immature nature of the sedimentary OM. The HI/OI and HI/Tmax plots indicate the presence of primarily Type III (gas prone) and Type IV (inert) kerogen in the samples. The Miocene Well D sediments with aquatic macroalgae-derived immature Type III kerogen and deposited under a C_3 marshy environment shows the presence of methanogenic archaea (*Methanocella* sp. and *Methanoformis* sp.) belong to hyperthermophilic groups and could contribute to the transformation of generated hydrocarbons into methane. Further study of the organic-rich deltaic Miocene successions is required for assessing the biogenic natural gas potential of the Indian (on-land) section of the Bengal Basin in West Bengal.

CRediT authorship contribution statement

Pravat Kumar Behera: Writing – original draft, Formal analysis. **Supriyo Kumar Das:** Conceptualization, Methodology, Validation, Investigation, Resources, Writing – original draft, Visualization, Supervision, Project administration, Funding acquisition. **Devanita Ghosh:** Writing – review & editing, Formal analysis. **Devleena Mani:** Formal analysis. **M.S. Kalpana:** Formal analysis. **Minoru Ikehara:** Formal analysis. **Priyank Pravin Patel:** Writing – review & editing.

Declaration of Competing Interest

The authors declare that they have no known competing financial interests or personal relationships that could have appeared to influence the work reported in this paper.

Acknowledgements

The Directorate General of Hydrocarbons is acknowledged for granting permission for receiving samples from the ONGC (DGH/G&G Data for Research Proposal/2015 dated 13 October 2015). KDMIPE and ONGC are acknowledged for providing samples. Mr B.M. Tripathy is acknowledged for assisting with sample selection and for necessary permissions. Department of Science and Technology (DST), Government of West Bengal (Memo No: 173(Sanc.)/ST/P/S&T/10G-23/2017) is acknowledged for providing funding for the research. The Council of Scientific & Industrial Research-Human Resource Development Group (CSIR-HRDG) is acknowledged for granting the fellowship (Junior Research Fellowship; File No: 08/155(0072)/2019-EMR-I) to Pravat Kumar Behera. Suggestions from John K. Volkman, Philip Meyers and an anonymous reviewer improved the manuscript.

Appendix A. Supplementary material

Supplementary data to this article can be found online at https://doi.org/10.1016/j.orggeochem.2022.104451.

References

Akbar, M.A., 2011. An assessment of the geothermal potential of Bangladesh. Geothermal Training Programme, Orkustofnun, Iceland. Reports, Number 5.
Alam, M., 1989. Geology and depositional history of Cenozoic sediments of the Bengal Basin of Bangladesh. Palaeogeography Palaeoclimatology Palaeoecology 69, 125–139.
Alam, M.M., 1995. Tide-dominated sedimentation in the upper Tertiary succession of the sitapahar anticline, Bangladesh. In: Flemming, B.W., Bortholma, A. (Eds.), Tidal Signatures in Modern and Ancient Sediments, vol. 24. Special Publications of the International Association of Sedimentologists, pp. 329–341.
Alam, M., Alam, M.M., Curray, J.R., Chowdhury, M.L.R., Gani, M.R., 2003. An overview of the sedimentary geology of the Bengal basin in relation to the regional tectonic framework and basin-fill history. Sedimentary Geology 155, 179–208.
Alexander, R., Kagi, R., Woodhouse, G.W., 1981. Geochemical correlation of Windalia oil and extracts of winning group (Cretaceous) potential source rocks, Barrow Subbasin, Western Australia. American Association of Petroleum Geologists Bulletin 65, 235–250.
Allison, M.A., 1998. Geologic framework and environmental status of the Ganges-Brahmaputra Delta. Journal of Coastal Research 14, 826–836.
Babu, P.V.L.P.A., 1976. A review on the oil & gas prospects of the Bengal basin based on photogeomorphological studies. Journal of the Indian Society of Photo-Interpretation 4, 1–13.
Banerji, R.K., 1984. Post-Eocene biofacies, palaeoenvironments and palaeogeography of the Bengal basin, India. Palaeogeography Palaeoclimatology Palaeoecology 45, 49–73.
Banerji, B., Ghosh, A., Pal, A.K., 1990. Eocene fossil algae from the subcrops of the Bengal Basin. Journal of the Palaeontological Society of India 35, 131–136.
Bastia, R., 2006. An overview of Indian sedimentary basins with special focus on emerging east coast deepwater frontiers. The Leading Edge 25, 818–829.
Basu, T.K., 1962. Subsurface Geology of the Indo-Stanvac concession, West-Bengal. In: Proceedings of the Seminar on oil prospects in the Ganga Valley, Oil & Natural Gas Commission, Dehradun, pp. 25–27.
Basu, S., Argawal, S., Sanyal, P., Mahato, P., Kumar, S., Sarkar, A., 2015. Carbon isotopic ratios of modern C_3–C_4 plants from the Gangetic Plain, India and its implications to paleovegetational reconstruction. Palaeogeography, Palaeoclimatology, Palaeoecology 440, 22–32.
Bedard-Haughn, A., van Groenigen, J.W., Van Kessel, C., 2003. Tracing ^{15}N through landscapes: potential uses and precautions. Journal of Hydrology 272, 175–190.
Behar, F., Beaumont, V., Penteado, H.D.B., 2001. Rock-Eval 6 technology: performances and developments. Oil & Gas Science and Technology 56, 111–134.
Berberich, M.E., Beaulieu, J.J., Hamilton, T.L., Waldo, S., Buffam, I., 2020. Spatial variability of sediment methane production and methanogen communities within a eutrophic reservoir: Importance of organic matter source and quantity. Limnology and oceanography 65, 1336–1358.
Billings, S.A., Richter, D.D., 2006. Changes in stable isotopic signatures of soil nitrogen and carbon during 40 years of forest development. Oecologia 148, 325–333.
BOGMC, 1997. Petroleum exploration opportunities in Bangladesh. Bangladesh Oil, Gas and Mineral Corporation (Petrobangla), Dhaka.
Boreham, C.J., Powell, T.G., 1993. Petroleum source rock potential of coal and associated sediments: qualitative and quantitative aspects. In: Law, B.E., Rice, D.D. (Eds.), Hydrocarbons from Coal, American Association of Petroleum Geologists Studies in Geology, vol. 38, pp. 133–157.
Bouloubassi, I., Guehenneux, G., Rullkötter, J., 1998. Biological marker significance of organic matter in sapropels from the Mediterranean ridge, Site 969. In: Proceedings of the Ocean Drilling Program, Scientific Results, pp. 261–270.
Bourbonniere, R.A., Meyers, P.A., 1996. Sedimentary geolipid records of historical changes in the water sheds and productivities of Lakes Ontario and Erie. Limnology and Oceanography 41, 352–359.
Bush, R.T., McInerney, F.A., 2013. Leaf wax *n*-alkane distributions in and across modern plants: Implications for paleoecology and chemotaxonomy. Geochimica et Cosmochimica Acta 117, 161–179.
Cai, Y., Guo, L., Wang, X., Aiken, G., 2015. Abundance, stable isotopic composition, and export fluxes of DOC, POC, and DIC from the Lower Mississippi River during 2006–2008. Journal of Geophysical Research: Biogeosciences 120, 2273–2288.
Careddu, G., Costantini, M.L., Calizza, E., Carlino, P., Bentivoglio, F., Orlandi, L., Rossi, L., 2015. Effects of terrestrial input on macro benthic food webs of the coastal sea are detected by stable isotope analysis in Gaeta Gulf. Estuarine, Coastal and Shelf Science 154, 158–168.
Cerling, T.E., Harris, J.M., 1999. Carbon isotope fractionation between diet and bioapatite in ungulate mammals and implications for ecological and paleoecological studies. Oecologia 120, 347–363.
Cernusak, L.A., Ubierna, N., Winter, K., Holtum, J.A., Marshall, J.D., Farquhar, G.D., 2013. Environmental and physiological determinants of carbon isotope discrimination in terrestrial plants. New Phytologist 200, 950–965.
Chandra, M., Mallik, S., Das, D., Thakur, R.K., Sinha, M.K., 1993. Lithostratigraphy of Indian Petroliferous Basins: Document IX, West Bengal Basin, KDMIPE, ONGC (Spec. Publ.), Dehradun, p. 216.

Craine, J.M., Brookshire, E.N.J., Cramer, M.D., Hasselquist, N.J., Koba, K., Marin-Spiotta, E., Wang, L., 2015. Ecological interpretations of nitrogen isotope ratios of terrestrial plants and soils. Plant and Soil 396, 1–26.
Curray, J.R., 1991. Geological history of the Bengal geosyncline. Journal of Association of Exploration Geophysicists XII 209–219.
Curray, J.R., Munasinghe, T., 1991. Origin of the Rajmahal Traps and the 85jE Ridge: preliminary reconstructions of the trace of the Crozet hotspot. Geology 19, 1237–1240.
Das, S.K., Routh, J., Roychoudhury, A.N., Klump, J.V., 2008. Elemental (C, N, H, and P) and stable isotope ($\delta^{15}N$ and $\delta^{13}C$) signatures in sediments from Zeekoevlei, South Africa: a record of human intervention in the lake. Journal of Paleolimnology 39, 349–360.
Das, S.K., Routh, J., Roychoudhury, A.N., 2009. Biomarker evidence of macrophyte and plankton community changes in Zeekoevlei, a shallow lake in South Africa. Journal of Paleolimnology 41, 507–521.
del Giorgio, P.A., Davis, J., 2003. Patterns in dissolved organic matter lability and consumption across aquatic ecosystems. In: Aquatic ecosystems. Academic Press, pp. 399–424.
Desikachar, O.S.V., 1974. A review of the tectonic and geological history of eastern India in terms of 'plate tectonics' theory. Journal of the Geological Society of India 33, 137–149.
Didyk, B.M., Simoneit, B.R.T., Brassell, S.C., Eglinton, G., 1978. Organic geochemical indicators of palaeoenvironmental conditions of sedimentation. Nature 272, 216–222.
Diefendorf, A.F., Mueller, K.E., Wing, S.L., Koch, P.L., Freeman, K.H., 2010. Global patterns in leaf ^{13}C discrimination and implications for studies of past and future climate. Proceedings of the National Academy of Sciences of the United States of America 107, 5738–5743.
Directorate General of Hydrocarbon, 2019. India's hydrocarbon outlook, 2018-19, a report on exploration & production activites.
Eglinton, G., Hamilton, R.J., 1967. Leaf epicuticular waxes. Science 156, 1322–1335.
Ficken, K.J., Li, B., Swain, D.L., Eglinton, G., 2000. An *n*-alkane proxy for the sedimentary input of submerged/floating freshwater aquatic macrophytes. Organic Geochemistry 31, 745–749.
France-Lanord, C., Derry, L.A., 1994. $\delta^{13}C$ of organic carbon in the Bengal Fan: source evolution and transport of C3 and C4 plant carbon to marine sediments. Geochimica et Cosmochimica Acta 58, 4809–4814.
Galman, V., Rydberg, J., Bigler, C., 2009. Decadal diagenetic effects on $\delta^{13}C$ and $\delta^{15}N$ studied in varved lake sediment. Limnology and Oceanography 54, 917–924.
Galy, V., France-Lanord, C., Peucker-Ehrenbrinkm, B., Huyghem, P., 2010. Sr-Nd-Os evidence for a stable erosion regime in the Himalaya during the past 12 Myr. Earth and Planetary Science Letters 290, 474–480.
Högberg, P., 1990. Forests losing large quantities of nitrogen have elevated ^{15}N:^{14}N ratios. Oecologia 84, 229–231.
Hossain, M., Khan, M., Hossain, S., Chowdhury, K.R., Abdullah, R., 2019. Synthesis of the tectonic and structural elements of the Bengal Basin and its surroundings. In: Tectonics and Structural Geology: Indian Context. Springer, Cham, pp. 135–218.
Hossain, H.M.Z., Sampei, Y., Roser, B.P., 2009. Characterization of organic matter and depositional environment of Tertiary mudstones from the Sylhet Basin, Bangladesh. Organic Geochemistry 40, 743–754.
Huber, T., Faulkner, G., Hugenholtz, P., 2004. Bellerophon: a program to detect chimeric sequences in multiple sequences alignments. Bioinformatics 20, 2317–2319.
Imam, B.I., Hussain, M., 2002. A review of hydrocarbon habitats in Bangladesh. Journal of Petroleum Geology 25, 31–52.
Islam, M.A., 2009. Diagenesis and reservoir quality of Bhuban sandstones (Neogene), Titas Gas Field, Bengal Basin, Bangladesh. Journal of Asian Earth Sciences 35, 89–100.
Jeng, W.-L., 2006. Higher plant *n*-alkanes average chain length as an indicator of petrogenic hydrocarbon contamination in marine sediments. Marine Chemistry 102, 242–251.
Johnson, S.Y., Alam, A.M.N., 1991. Sedimentation and tectonics of the Sylhet Trough, Bangladesh. Geological Society of America Bulletin 103, 1513–1527.
Jones, D.T., Taylor, W.R., Thornton, J.M., 1992. The rapid generation of mutation data matrices from protein sequences. Bioinformatics 8, 275–282.
Kellerman, A.M., Guillemette, F., Podgorski, D.C., Aiken, G.R., Butler, K.D., Spencer, R. G., 2018. Unifying concepts linking dissolved organic matter composition to persistence in aquatic ecosystems. Environmental Science & Technology 52, 2538–2548.
Kemp, A.C., Vane, C.H., Horton, B.P., Engelhart, S.E., Nikitina, D., 2012. Application of stable carbon isotopes for reconstructing salt-marsh floral zones and relative sea level, New Jersey, USA. Journal of Quaternary Science 27, 404–414.
Khan, N.S., Vane, C.H., Horton, B.P., 2015. Stable carbon isotope and C/N geochemistry of coastal wetland sediments as a sea-level indicator. In: Handbook of Sea-Level Research. John Wiley & Sons Ltd, pp. 295–311.
Kohn, M.J., 2010. Carbon isotope compositions of terrestrial C_3 plants as indicators of (paleo)ecology and (paleo)climate. Proceedings of the National Academy of Sciences of the United States of America 107, 19691–19695.
Kumar, S., Stecher, G., Tamura, K., 2016. MEGA7: Molecular Evolutionary Genetics Analysis version 7.0 for bigger datasets. Molecular Biology and Evolution 33, 1870–1874.
Kuramoto, T., Minagawa, M., 2001. Stable carbon and nitrogen isotopic characterization of organic matter in a mangrove ecosystem on the southwestern coast of Thailand. Journal of Oceanography 57, 421–431.
Lafargue, E., Marquis, F., Pillot, D., 1998. Rock-Eval 6 applications in hydrocarbon exploration, production, and soil contamination studies. Revue de l'institut français du pétrole 53, 421–437.
Laier, T., Jorgensen, N.O., Buchardt, B., Cederberg, T., Kuijpers, A., 1992. Accumulation and seepages of biogenic gas in Northern Denmark. Continental Shelf Research 12, 1173–1186.
Lehmann, M.F., Bernasconi, S.M., Barbieri, A., McKenzie, J.A., 2002. Preservation of organic matter and alteration of its carbon and nitrogen isotope composition during simulated and in situ early sedimentary diagenesis. Geochimica et Cosmochimica Acta 66, 3573–3584.
Li, M.W., Larter, S.R., Taylor, P., Jones, D.M., Bowler, B., Bjorøy, M., 1995. Biomarkers or not biomarkers? A new hypothesis for the origin of pristine involving derivation from methyltrimethyltridecylchromans (MTTCs) formed during diagenesis from chlorophyll and alkylphenols. Organic Geochemistry 23, 159–167.
Li, Y., Zhang, H., Tu, C., Fu, C., Xue, Y., Luo, Y., 2016. Sources and fate of organic carbon and nitrogen from land to ocean: Identified by coupling stable isotopes with C/N ratio. Estuarine, Coastal and Shelf Science 181, 114–122.
Lijmbach, W., 1975. On the origin of petroleum. 9th World Petroleum Congress.
Liles, M.R., Williamson, L.L., Rodbumrer, J., Torsvik, V., Parsley, L.C., Goodman, R.M., Handelsman, J., 2009. Isolation and cloning of high molecular weight metagenomic DNA from soil microorganisms. Cold Spring Harbor Protocols 4, 1024–1032.
Littke, R., Leythaeuser, D., 1993. Migration of oil and gas in coals. American Association of Petroleum Geologists Bulletin 38, 219–236.
Luton, P.E., Wayne, J.M., Sharp, R.J., Riley, P.W., 2002. The *mcrA* gene as an alternative to 16S rRNA in the phylogenetic analysis of methanogen populations in landfill. Microbiology 148, 3521–3530.
Madeira, F., Park, Y.M., Lee, J., Buso, N., Gur, T., Madhusoodanan, N., Basutkar, P., Tivey, A.R.N., Potter, S.C., Finn, R.D., Lopez, R., 2019. The EMBL-EBI search and sequence analysis tools APIs in 2019. Nucleic Acids Research 47, W636–W641.
Mauerhofer, L.M., Zwirtmayr, S., Pappenreiter, P., Bernacchi, S., Seifert, A.H., Reischl, B., Schmider, T., Taubner, R.S., Paulik, C., Rittmann, S.K.M., 2021. Hyperthermophilic methanogenic archaea act as high-pressure CH4 cell factories. Communications Biology 4, 1–12.
Meyer, B., Kuever, J., 2007. Molecular analysis of the diversity of sulfate-reducing and sulphur-oxidizing prokaryotes in the environment, using aprA as functional marker gene. Applied and Environmental Microbiology 73, 7664–7679.
Meyers, P.A., 1994. Preservation of elemental and isotopic source identification of sedimentary organic matter. Chemical Geology 114, 289–302.
Meyers, P.A., 1997. Organic geochemical proxies of paleoceanographic, paleolimnologic and paleoclimatic processes. Organic Geochemistry 27, 213–250.
Meyers, P.A., Ishiwatari, R., 1993. Lacustrine organic geochemistry–an overview of indicators of organic matter sources and diagenesis in lake sediments. Organic Geochemistry 20, 867–900.
Meyers, P.A., Teranes, J.L., 2001. Sediment organic matter. In: Last, W.M., Smol, J.P. (Eds.), Tracking Environmental Change using Lake Sediments, Physical and Geochemical Methods, vol. 2. Kluwer Academic Publishers, Dordrecht, pp. 239–269.
Middelburg, J.J., Herman, P.M.J., 2007. Organic matter processing in tidal estuaries. Marine Chemistry 106, 127–147.
Möbius, J., Lahajnar, N., Emeis, K.C., 2010. Diagenetic control of nitrogen isotope ratios in Holocene sapropels and recent sediments from the Eastern Mediterranean Sea. Biogeosciences 7, 3901–3914.
Morgan, J.P., McIntire, W.G., 1959. Quaternary geology of the Bengal Basin (East Pakistan and India). Geological Society of America Bulletin 70, 319–342.
Mukherjee, A., Fryar, A.E., Thomas, W.A., 2009. Geologic, geomorphic and hydrologic framework and evolution of the Bengal basin, India and Bangladesh. Journal of Asian Earth Sciences 34, 227–244.
Najman, Y., Bickle, M., BouDagher-Fadel, M., Carter, A., Garzanti, E., Paul, M., Wijbrans, J., Willett, E., Oliver, G., Parrish, R., Akhter, S.H., Allen, R., Ando, S., Chisty, E., Reisberg, L., Vezzoli, G., 2008. The Paleogene record of Himalayan erosion: Bengal Basin, Bangladesh. Earth and Planetary Science Letters 273, 1–14.
Natelhoffer, K.J., Fry, B., 1988. Controls on natural nitrogen-15 and carbon-13 abundances in forest soil organic matter. Soil Science Society of America 52, 1633–1640.
Nguyen, R.T., Harvey, H.R., 1997. Protein and amino acid cycling during phytoplankton decomposition in oxic and anoxic waters. Organic Geochemistry 27, 115–128.
Oremland, R.S., Polcin, S., 1982. Methanogenesis and sulfate reduction: competitive and noncompetitive substrates in estuarine sediments. Applied and Environmental Microbiology 44, 1270–1276.
Ortiz, J.E., Moreno, L., Torres, T., Vegas, J., Ruiz-Zapata, B., Garcia-Cortes, A., Galan, L., Perez-Gonzalez, A., 2013. A 220 ka paleoenvironmental reconstruction of the Fuentillejo maar lake record (central Spain) using biomarker analysis. Organic Geochemistry 55, 85–97.
Peters, K.E., 1986. Guidelines for evaluating petroleum source rock using programmed pyrolysis. American Association of Petroleum Geologists Bulletin 70, 318–386.
Peters, K.E., Clark, M.E., Das Gupta, U., McCaffrey, M.A., Lee, C.Y., 1995. Recognition of an infraCambrian source rock based on biomarkers in the Bagehwala-1 oil, India. American Association of Petroleum Geologists Bulletin 79, 1481–1494.
Peters, K.E., Fraser, T.H., Amris, W., Rustanto, B., Hermanto, E., 1999. Geochemistry of crude oils from eastern Indonesia. American Association of Petroleum Geologists Bulletin 83, 1927–1942.
Peters, K.E., Walters, C.C., Moldowan, J.M., 2005. The Biomarker Guide. Biomarkers and Isotopes in the Environment and Human History. Cambridge University Press, New York. Chapter 4.
Ramaswamy, G., 1962. Aeromagnetic and gravity surveys of West Bengal. In: Proceedings of the Seminar on oil prospects in the Ganga Valley. Oil and Natural Gas Corporation, Dehradun, pp. 28–29.
Ramaswamy, V., Gaye, B., Shirodkar, P.V., Rao, P.S., Chivas, A.R., Wheeler, D., Thwin, S., 2008. Distribution and sources of organic carbon, nitrogen and their

isotopic signatures in sediments from the Ayeyarwady (Irrawaddy) continental shelf, northern Andaman Sea. Marine Chemistry 111, 137–150.
Rea, D.K., 1992. Delivery of the Himalayan sediments to the Northern Indian Ocean and its relation to global climate, sea-level, uplift and sea water strontium. In: Duncan, R. A., Rea, D.K., Kidd, R.B., von Rad, U., Weissel, J.K. (Eds.), Synthesis of Results from Scientific Drilling in the Indian Ocean, vol. 70. American Geophysical Union, Washingto, DC, pp. 387–402.
Rice, P., Longden, I., Bleasby, A., 2000. EMBOSS: the European molecular biology open software suite. Trends in Genetics 16, 276–277.
Rieley, G., Collier, R.J., Jones, D.M., Eglinton, G., Eakin, P.A., Fallick, A.E., 1991. Sources of sedimentary lipids deduced from stable carbon-isotope analyses of individual compounds. Nature 352, 425–427.
Rontani, J.F., Bonin, P., 2011. Production of pristane and phytane in the marine environment: role of prokaryotes. Research in Microbiology 162, 923–933.
Roy, A.B., Chatterjee, A., 2015. Tectonic framework and evolutionary history of the Bengal Basin in the Indian subcontinent. Current Science 271–279.
Roybarman, A., 1984. Geology and hydrocarbon prospects of West Bengal. Petroleum Asia Journal 6, 51–56.
Saitou, N., Nei, M., 1987. The neighbor-joining method: a new method for reconstructing phylogenetic trees. Molecular Biology and Evolution 4, 406–425.
Sakai, S., Conrad, R., Liesack, W., Imachi, H., 2010. *Methanocella arvoryzae* sp. nov., a hydrogenotrophic methanogen isolated from rice field soil. International Journal of Systematic and Evolutionary Microbiology 60, 2918–2923.
Sakata, S., Hayes, J.M., McTaggart, A.R., Evans, R.A., Leckrone, K.J., Togasaki, R.K., 1997. Carbon isotopic fractionation associated with lipid biosynthesis by a cyanobacterium: relevance for interpretation of biomarker records. Geochimica et Cosmochimica Acta 61, 5379–5389.
Schelske, C.L., Hodell, D.A., 1995. Using carbon isotopes of bulk sedimentary organic matter to reconstruct the history of nutrient loading and eutrophication in Lake Erie. Limnology and Oceanography 409, 918–929.
Sengupta, S., 1966. Geological and geophysical studies in western part of Bengal Basin, India. American Association of Petroleum Geologists Bulletin 50, 1001–1017.
Shamsuddin, A.H.M., Khan, S.I., 1991. Geochemical criteria of migration of natural gases in the Miocene sediments of the Bengal Foredeep, Bangladesh. Journal of Southeast Asian Earth Sciences l5, 89–100.
Silliman, J.E., Meyers, P.A., Bourbonniere, R.A., 1996. Record of postglacial organic matter delivery and burial in sediments of Lake Ontario. Organic Geochemistry 24, 463–472.
Tareq, S.M., Tanoue, E., Tsuji, H., Tanaka, N., Ohta, K., 2005. Hydrocarbon and elemental carbon signatures in a tropical wetland: biogeochemical evidence of forest fire and vegetation changes. Chemosphere 59, 1655–1665.
ten Haven, H.L., de Leeuw, J.W., Rullkötter, J., Sinninghe Damsté, J.S., 1987. Restricted utility of the pristane/phytane ratio as a palaeoenvironmental indicator. Nature 330, 641–643.
Teranes, J.L., Bernasconi, S.M., 2000. The record of nitrate utilization and productivity limitation provided by δ15N values in lake organic matter—A study of sediment trap and core sediments from Baldeggersee, Switzerland. Limnology and Oceanography 45, 801–813.
Tewari, A., Dutta, S., Sarkar, T., 2017. Biomarker signatures of Permian Gondwana coals from India and their palaeobotanical significance. Palaeogeography, Palaeoclimatology, Palaeoecology 468, 414–426.
Thauer, R.K., 1998. Biochemistry of methanogenesis: a tribute to Marjory Stephenson. 1998 Marjory Stephenson Prize Lecture. Microbiology 144, 2377–2406.
Tissot, B.P., Welte, D.H., 1984. Petroleum Formation and Occurrence, second ed. Springer-Verlag, Berlin.
Tringe, G.S., Rubin, E.M., 2005. Metagenomics: DNA sequencing of environmental samples. Nature Reviews Genetics 6, 805–814.
Uddin, A., 1990. Shift in depositional patterns during Miocene time in the Bengal Basin, Bangladesh. Geological Society of America Program with Abstracts 22, A366.
Uddin, A., Lundberg, N., 1998. Cenozoic history of the Himalayan-Bengal system: sand composition in the Bengal basin, Bangladesh. Geological Society of America Bulletin 110, 497–511.
Volkman, J.K., Barrett, S.M., Blackburn, S.I., Mansour, M.P., Sikes, E.L., Gelin, F., 1998. Microalgal biomarkers: a review of recent research developments. Organic Geochemistry 29, 1163–1179.
Walker, D.I., McComb, A.J., 1985. Decomposition of leaves from *Amphibolis antarctica* (Labill.) Sonder ex Aschers. and *Posidonia australis* Hook. f. the major seagrasses of Shark Bay. Western Australia. Botanica Marina 28, 407–413.
Wu, W., Ruan, J., Ding, S., Zhao, L., Xu, Y., Yang, H., Ding, W., Pei, Y., 2014. Source and distribution of glycerol dialkyl glycerol tetraethers along lower Yellow River-estuary–coast transect. Marine Chemistry 158, 17–26.
Wynn, J.G., Bird, M.I., 2007. C_4-derived soil organic carbon decomposes faster than its C_3 counterpart in mixed C_3/C_4 soils. Global Change Biology 13, 2206–2217.
Xing, L., Zhang, H., Yuan, Z., Sun, Y., Zhao, M., 2011. Terrestrial and marine biomarker estimates of organic matter sources and distributions in surface sediments from the East China Sea shelf. Continental Shelf Research 31, 1106–1115.
Yakimovich, K.M., Emilson, E.J., Carson, M.A., Tanentzap, A.J., Basiliko, N., Mykytczuk, N., 2018. Plant litter type dictates microbial communities responsible for greenhouse gas production in amended lake sediments. Frontiers in Microbiology 2662.
Yakimovich, K.M., Orland, C., Emilson, E.J., Tanentzap, A.J., Basiliko, N., Mykytczuk, N., 2020. Lake characteristics influence how methanogens in littoral sediments respond to terrestrial litter inputs. The ISME Journal 14, 2153–2163.
Zhang, Z., Zhao, M., Yang, X., Wang, S., Jiang, X., Oldfield, F., Eglinton, G., 2004. A hydrocarbon biomarker record for the last 40 kyr of plant input to Lake Heqing, southwestern China. Organic Geochemistry 35, 595–613.